International
Progress Report

IPR-02-16

# Äspö Hard Rock Laboratory

## TRUE Block Scale project

## Investigation of the correlation between early-time hydraulic response and tracer breakthrough times in fractured media

Benoit Paris

Itasca Consultants S.A.

October 2002

**Svensk Kärnbränslehantering AB**
Swedish Nuclear Fuel
and Waste Management Co
Box 5864
SE-102 40 Stockholm Sweden
Tel +46 8 459 84 00
Fax +46 8 661 57 19

Äspö Hard Rock
Laboratory

| Report no. | No. |
| --- | --- |
| IPR-02-16 | F56K |
| Author | Date |
| Benoit Paris | Oct 2002 |
| Checked by | Date |
| Anders Winberg | Jan 2003 |
| Approved | Date |
| Christer Svemar | 03-04-16 |

# Äspö Hard Rock Laboratory

## TRUE Block Scale project

## Investigation of the correlation between early-time hydraulic response and tracer breakthrough times in fractured media

Benoit Paris

Itasca Consultants S.A.

October 2002

*Keywords:* Breakthrough, correlation, drawdown, early time, fracture, network, tracer test

# ABSTRACT

ITASCA has been participating in the TRUE Block Scale experiment since its start, conducted at the Äspö Hard Rock Laboratory in Sweden. An objective of this experiment was to detect and characterize retention effects at a scale such that a network of fractures, and not only a single fracture, is concerned.

Previous work in porous-media hydrogeology (Herweijer, 1996) showed a correlation between the early-time response to pumping tests and tracer first arrival times. The author explained this by the fact that pumping test data reveal high conductivity inter-well pathways, which dominate the solute transport in the aquifer considered. In fractured rock, where flowpath conductivities are generally highly variable, this is also likely to be the case.

The aim of this project was to investigate the existence and relevance of this correlation in fracture networks, focusing on the understanding of the response of the system modeled, in order to check the robustness of the "drawdown-breakthrough time" relationship. The final objective was to assess if this concept could be of use to help dimensioning transport experiments All the simulations used the TRUE Block Scale hydrostructural model as the base case reference.

A constant-head test (50 m draw-down at pumping well) and advective tracer tests in various fracture networks were simulated changing both network geometry and conductor hydraulic properties. The breakthrough time for a 0.5 cm drawdown (1/1000) and the arrival time for 1 % of the tracer were then compared.

We showed that the correlation of pressure and tracer breakthroughs described by Herweijer (1996) should normally have been expected in an homogeneous system or equivalent. The shape of this correlation is a straight-line with a slope close to 1. The line position on the plan depends on the system specific storage and porosity.

In a fractured medium, the system geometry has a major influence on the quality of the correlation by eventually adding some extra tracer dispersion to the transport pathways. It appeared that the correlation was all the more altered if the pathways between the injection / recovery wells involved crossing a high number of fracture intersections. If varying global system conductivities do not affect the correlation, it is likely that a variable conductivity inside each fracture would influence the results.

Matrix diffusion or any non-linear retardation phenomenon might also affect the correlation but to a much lesser extent, essentially because we track the early pressure response and early tracer breakthroughs.

In terms of practical application of the concepts discussed in this report, good results can be expected if the distance between the monitoring and the pumping wells is not too large. Beside increasing the test durations, increasing distances between wells may add fracture intersections and complexity into the flow and transport system and result into poorer correlations.

# SAMMANFATTNING

Målet med TRUE Block Scale-projektet som genomförs i Äspölaboratoriet är att identifiera och karakterisera effekter av retention av spårämnen på en sådan skala att inte endast en enskild spricka berörs, utan ett nätverk av sprickor. Tidigare arbete inom hydrogeologi i porösa medier (Herweijer, 196) har påvisat en korrelation mellan tidig avsänkning i observationsborrhål i samband med hydrauliska tester (provpumpning) och tidpunkten för första genombrott observerad i samband med spårförsök mellan motsvarande borrhål. Författaren förklarade denna observation som ett resultat av att provpumpningen kartlägger hög-konduktiva flödesvägar mellan borrhålen som även dominerar transport i den studerade akvifären. I kristallint berg, där den hydrauliska konduktiviteten generellt är mycket variabel, förväntas dock samma förhållande råda. Målet för den utförda modellstudien har varit att undersöka förekomst och relevans av den framförda korrelationen för nätverk av strukturer/sprickor. Speciell vikt har lagts på förståelsen av responsen av det modellerade systemet för att undersöka hur pass robust sambandet mellan ”avsänkning och ankomsttid” är. Ett ytterligare mål är att utreda om det studerade konceptet kan användas i design och dimensionering av spårförsök. Den aktuella studien genomfördes med den beskrivande, hydrostrukturella modellen som referensfall. En provpumpning med konstant avsänkning (50 m avsänkning i pumpsektionen) och ett spårförsök simulerades med koden 3FLO i olika spricknätverk där både geometri och egenskaper hos ingående sprickor tilläts variera. Tidpunkten för en avsänkning i observationssektionen på 0,5 cm (1 promille av avsänkningen i pumpsektionen) och tidpunkten för genombrott av 1% av den injicerade massan (antal partiklar) noterades och jämfördes. Det påvisades att den noterade korrelation mellan avsänkning och genombrott som beskrivits av Herweijer (1996) normalt skall förväntas i ett homogent system. Formen på sambandet är en rät linje med en lutning på nära 1. Den utbildade korrelationen beror dock på systemets specifika magasinskoefficient och porositet. I kristallint berg har det studerade systemets geometri en avgörande betydelse för graden av korrelation genom att ett extra element av dispersion introduceras i de utvecklade transportvägarna. Det påvisades att korrelationen förändrades i avgörande grad om transportvägarna mellan injicerings- och pumpsektion inkluderade korsade ett större antal skärningar mellan sprickor. Det förväntas att förändring av materialegenskaper inom varje spricka kommer att påverka den utbildade korrelationen. På samma sätt förväntas att matrisdiffusion, eller andra icke-linjära retentionsmekanismer, påverka korrelationen. Detta förväntas dock ske i mindre omfattning då företrädesvis tidiga tryckresponser och genombrott studeras. Vad avser praktisk tillämpning av koncept, diskuterade i denna studie, förväntas goda resultat (korrelation) då avståndet mellan observationsborrhål och pumpsektion inte är alltför stort. Bortsett från att transporttiderna blir längre så medverkar ett större avstånd till större komplexitet, och därmed försämrad korrelation.

# Contents

# LIST OF FIGURES



# LIST OF TABLES

# 1. INTRODUCTION

ITASCA has been participating in the TRUE Block Scale experiment since its start, conducted at the Äspö Hard Rock Laboratory in Sweden. An objective of this experiment is to detect and characterize retention effects at a scale such that a network of fractures, and not only a single fracture, is concerned.

A major difficulty in this experiment is dimensioning tracer tests so that time scales are:

- Long enough for the retention to take place;
- Short enough for the experiment to be feasible.

Being able to assess transport time scales before performing a full-scale experiment is therefore critical to the project.

Previous work in porous-media hydrogeology (Herweijer, 1996) shows a correlation between the early-time response to pumping tests and tracer first arrival times. The author explains this by the fact that pumping test data reveal high conductivity inter-well pathways, which dominate the solute transport in the aquifer being considered. In fractured rock, where flowpath hydraulic conductivities generally are highly variable, this is also likely to be the case.

The aim of this project is to investigate the existence and relevance of this correlation in fracture networks, and to assess if this can be of use to help designing and predicting transport experiments. This report describes the results of this study that is focusing on the understanding of the response of the system modeled in order to check the robustness of the "drawdown-breakthrough time" relationship. Starting from the "TRUE Block Scale alike" network, we first study the effect of "network scale" (Chapter 2). For network properties such that the correlation is well verified, we then study the influence of the simulations (Chapter 3). Chapter 4 contains our conclusions.

# 2. GENERAL PRESENTATION, APPROACH AND NETWORKS TO BE STUDIED

## 2.1 Presentation

The approach of our study is the following:

- Generate fractured media with varying geometrical scales while keeping our base case as a reference;
- Perform numerical flow and transport experiments in the fracture networks;
- Interpret the simulated tests and check on the « flow-transport » correlation;

After outlining the conceptual model used, the "base" TRUE Block Scale network model is decribed. The way it is altered for studying the effect of "network scale", and the results of a parameter study are then presented and used to chose the networks of interest.

## 2.2 General characteristics of the 3FLO numerical models and of the transport simulations

For better understanding of the numerical models, a brief description of *3FLO* is described in Appendix.

Each model has a cylindrical shape (Figure 2-1) with a radius and a height of 50 m.

The initial pressure head is applied uniformly in the entire network at 50 m. It is fixed at 50 m on the circumference of the cylinder.

A vertical well, 6 cm radius, is placed in the center of each model. The well intersects the entire network. In order to remove numerical skin effects, the mesh is refined around the well. To do so, the pipes connected to the well are discretized in a succession of 15 pipes whose length increases geometrically with the distance to the central well.

The modeling of the fractures is identical for the different networks:

- Fractures are represented by discs;
- Disc radii are distributed according to a lognormal law (with truncation of the lowest conductivity values),
- Disc centers have random positions (Poisson point process);
- Pipes are generated according to a regular mesh on each fracture;
- Whenever a fracture disc crosses the central well, the pipe grid on the fracture is arranged so that it intersects the well.

***Figure 2-1:*** *Models geometry and boundary conditions*

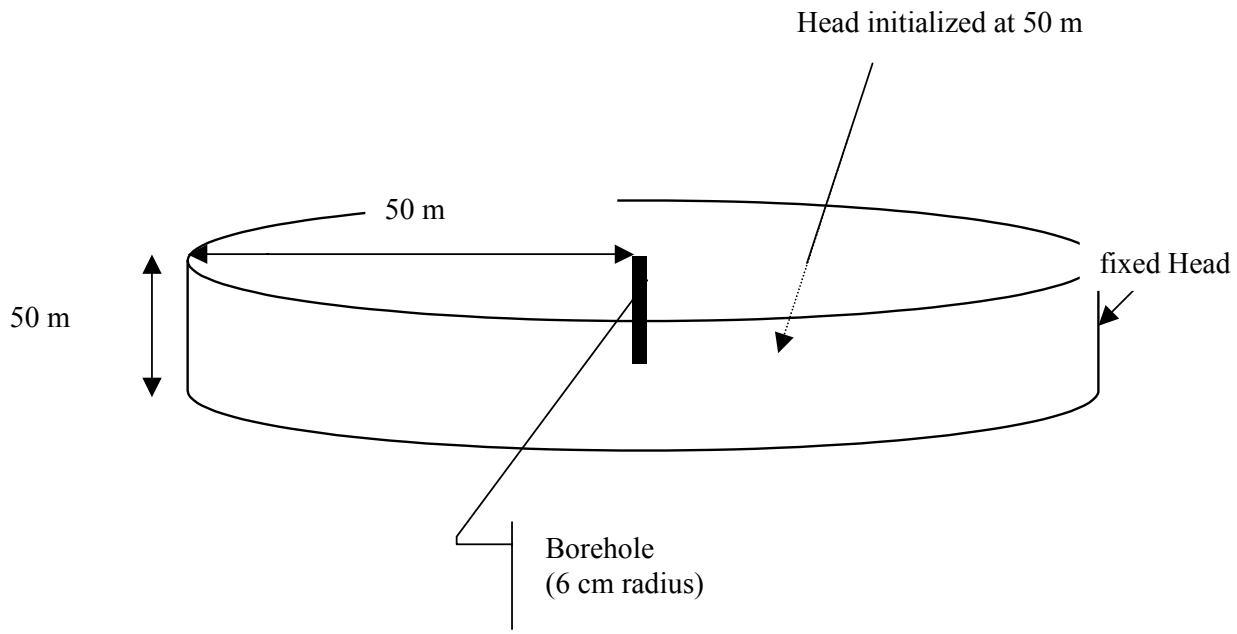

For each network the following entities are specified:

- Number of fractures sets;
- Average fracture orientation of each set;
- Center density;
- Parameters of the lognormal law for the fracture radii;
- Parameters of the lognormal law for the pipe conductivities. These parameters are fixed so as to obtain the macroscopic characteristics specified in the preceding studies of 1994 and 1997;

In each network, the pipe section A is either constant or correlated with conductivity C according to the law:

$$A = C^{1/3}$$

Several observation wells are defined in the network where head is monitored and where particles are injected. These observation wells are located at different radial distances from the central well.

A constant head test is first simulated. In this test, a 0 m head is imposed directly on the central well's circumference. A flow calculation is carried out in transient mode until at least a 1/1000 (i.e. 5 mm) decrease of the head is observed in the three observation wells. A steady state flow is then computed, 1000 particles are injected in each observation well and the transport simulation begins. The injected particles are marked and the time needed for a given particle to arrive into the central well is measured. We chose to plot the arrival time of the first 10 particles (1% of the injected mass). For each observation well point in a network we thus obtain a data pair: "time for which there is a 1/1000 decrease of the head" versus "time of particle arrivals".

## 2.3 Properties of the TRUE Block Scale background fractures

The parameters taken into account for the TRUE Block Scale geometrical model result from a previous study for ANDRA (Hermanson et al, 2001).

There are three sets of background fractures, their properties are given in Table 2-1. The interpreted deterministic structures are not taken into account.

**Table 2-1: Parameters of the TRUE Block Scale network**
(from Hermanson et al., 2001)

| Fracture set | Mean Orientation | | Lognormal distribution of the fractures radii | | Vol. Density |
|---|---|---|---|---|---|
| | Dip Dir. (Thêta, °) | Dip (phi, °) | Mean (m) | Sd-deviation (m) | Fractures/$m^3$ |
| 1 | 117.9 | 12.9 | 4 | 2 | (1.7/4) x dens_tot |
| 2 | 200.4 | 2.0 | 4 | 2 | (1.5/4) x dens_tot |
| 3 | 186.5 | 81.1 | 4 | 2 | (0.8/4) x dens_tot |
| with dens_tot = 6.0e-2 | | | | | |

The density of 6.0e-2 fractures/$m^3$ is very high. Generating the three sets of fractures in a volume that is large enough to do the transport simulations is above our current computer capacity.

We thus decrease the total density of fractures, while disturbing as little as possible the network properties, in two successive stages :

1) by discarding fractures with small fracture radii (while keeping the network connectivity constant),
2) by discarding fractures with low conductivities (while keeping the network permeability constant).

These two stages are described below.

*Statistical law for the radii:*

The connectivity of a network may be expressed in terms of a weighted mean number of intersections per fracture (Guérin and Billaux, 1993), with a network being able to percolate water at a large scale when this index is above 6, and any index above 20 denoting a very well connected network. Here, if the fracture radii are distributed according to the lognormal law from Table 2-1. (without truncation), the network connectivity is around 52,7. By removing all the fractures with a radius lower than 3 m, the network connectivity is 48,5 (-8%), which remains very comparable. As nearly 36,5% of the fractures have a radius lower than 3 m, we just have to generate the three fractures sets with a total fracture density of $3{,}82.10^{-2}$ fractures/$m^3$ while truncating them to 3 m, to obtain a network equivalent to the one given in Table 2-1.

*Statistical law for the conductivity:*

The pipe grid mesh on each fracture has a 5 m equidistance.
The pipe transmissivity distribution is lognormal. The associated normal law in $\log_{10}$ has a mean of –11 and a standard-deviation 1,7.

Conductivities are thus distributed in a first step according to the following lognormal law:

- Mean conductivity $1{,}39.10^{-9}$ $m^3/s$
- Standard-deviation $3{,}88.10^{-8}$ $m^3/s$
- no truncation

The permeability is calculated for three simulations of the TRUE Block Scale network.

By taking a sphere with a 16 m radius, and by calculating the flowrate through a 11 m radius disc, the permeability is $0.76.10^{-10}$ m/s (mean of the $K_1$, $K_2$ et $K_3$ permeabilities over the three realizations, (complete results in Table 2.2)).

The pipe conductivity distribution used on the fractures yields to a variation of the conductivity between $10^{-15.38}$ $m^3/s$ and $10^{-5.11}$ $m^3/s$, which is 10 orders of magnitude. 61,3% of the pipes have a conductivity between $10^{-10}$ $m^3/s$ and $10^{-15,38}$ $m^3/s$. These low conductivity pipes can be eliminated without drastically changing the flow. Those pipes are thus eliminated by truncating the conductivity distribution law at $10^{-10}$ $m^3/s$. The total density of fractures that have to be generated before truncation by the radii distribution law and the conductivity distribution law is then only $1,48.10^{-2}$ fract./$m^3$.

Another permeability calculation (Table 2.3) is done for three realizations of the TRUE Block Scale network with:

- distribution of the conductivity with a truncation at $10^{-10}$ $m^3/s$,
- distribution of the radii with a truncation at 3 m, and
- total fractures density of $1,48.10^{-2}$ fractures/$m^3$.

The global permeability is $0,73.10^{-10}$ m/s (average over the three realizations), which is very comparable to the permeability of $0,76.10^{-10}$ m/s obtained without truncating the conductivity.

We use these final characteristics (truncation of the radius and of the conductivity) to generate the TRUE Block Scale network in order to simulate transport.

The intrinsic storage coefficient $S_{si}$ is such that the specific storage $S_s$ of the network is $5.10^{-7}$ $m^{-1}$ and corresponds to what is estimated for the TRUE Block Scale site.

**Table 2-2: Permeability tensors for three simulations of the TRUE Block Scale network with a fracture density of $3,82.10^{-2}$ fract./$m^3$ (no truncation of the pipe conductivity) (simulation in a sphere with a 16 m radius)**

| Simulation number | Dip (angle phi) (°) | Dip Direct. (Thêta, °) | $K_1$ $K_2$ $K_3$ ($10^{-9}$ m/s) | Variability Index $I_v$ |
|---|---|---|---|---|
| 1 | 41,61 | -75,42 | 0,94 | |
| | 129,46 | -97,51 | 0,86 | 1,86E-03 |
| | 101,12 | 1,80 | 0,64 | |
| 2 | 24,22 | -60,19 | 0,90 | |
| | 113,07 | -78,91 | 0,61 | 9,56E-04 |
| | 96,96 | 14,07 | 0,56 | |
| 3 | 23,74 | -34,86 | 0,99 | |
| | 102,21 | -95,39 | 0,78 | 8,58E-04 |
| | 110,03 | -0,86 | 0,63 | |

**Table 2-3: Permeability tensors for three simulations of the TRUE Block Scale network with a fracture density of 1,48.$10^{-2}$ fract./$m^3$ (truncation of the pipe conductivity at $10^{-10}$ $m^3$/s (simulation in a sphere with a 16 m radius)**

| Simulation number | Dip (angle phi) (°) | Dip Direct. (Thêta, °) | $K_1$ $K_2$ $K_3$ ($10^{-9}$ m/s) | Variability Index $I_v$ |
|---|---|---|---|---|
| 1 | 11,1 | -123,3 | 0,77 | |
| | 95,7 | -63,7 | 0,66 | 5,76E-03 |
| | 80,5 | 25,4 | 0,44 | |
| 2 | 122,5 | -147,3 | 1,06 | |
| | 42,6 | -101,1 | 0,99 | 4,43E-03 |
| | 114,3 | -40,6 | 0,80 | |
| 3 | 33,6 | -50,0 | 0,73 | |
| | 104,4 | -117,3 | 0,65 | 6,45E-03 |
| | 119,6 | -18,9 | 0,41 | |

## 2.4 Influence of the scale effect

The aim here is to assess the influence of the scale of heterogeneity on the correlation between the pumping test response and the tracer breakthrough times. We compute the response of six networks, with various fracture density and fracture mean radius, everything else being kept constant. For all the networks, the product of the fracture density times the mean square fracture radius is kept constant. This fixes the average number of fractures a borehole would intersect (line density, or "fracture area per unit volume of the medium"). Therefore, all the networks would look identical if probed by boreholes : they conform to the most robust type of fracture statistic we have access to.

Figure 2-2 to Figure 2-7 show the results, for fracture mean radii varying from 3.2 m to 200 m. They show very clearly how the degree of correlation depends on the respective scale of the fractures and of the volume of rock tested. In other words, the correlation we are investigating may be of practical interest only if the flow paths tested include only a few fractures.

In view of these results, we chose to use two networks with fairly large mean radii, ie. 70 m and 140 m.

***Figure 2-2:*** *Head drawdown and tracer breakthroughs – Mean radius 3.2 m*

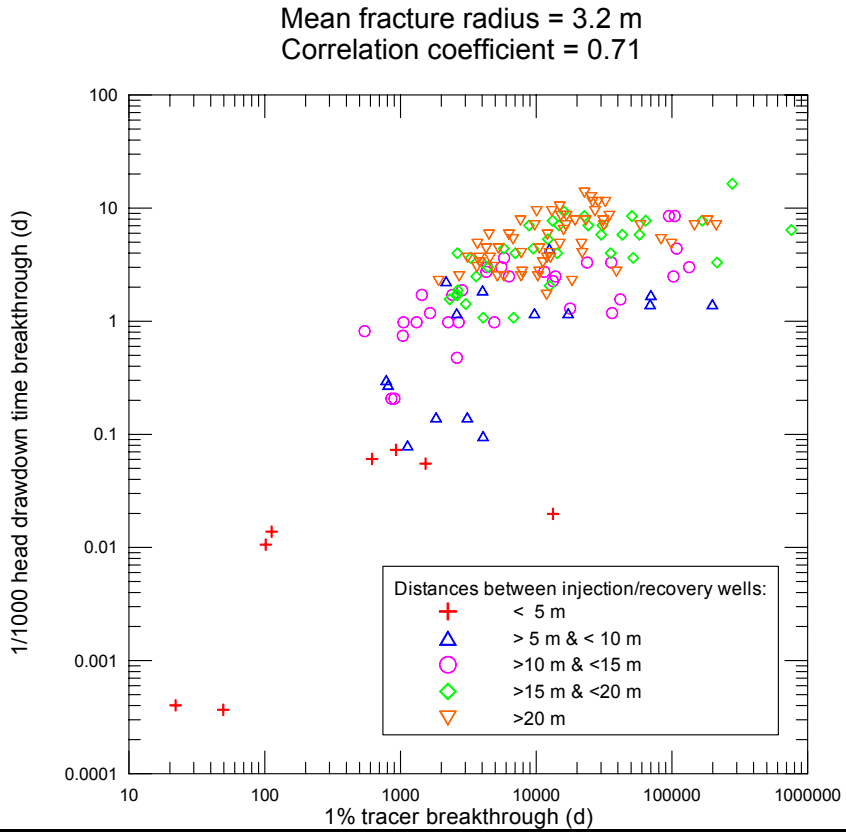


***Figure 2-3:*** *Correlation plot – Mean radius 6.3 m*

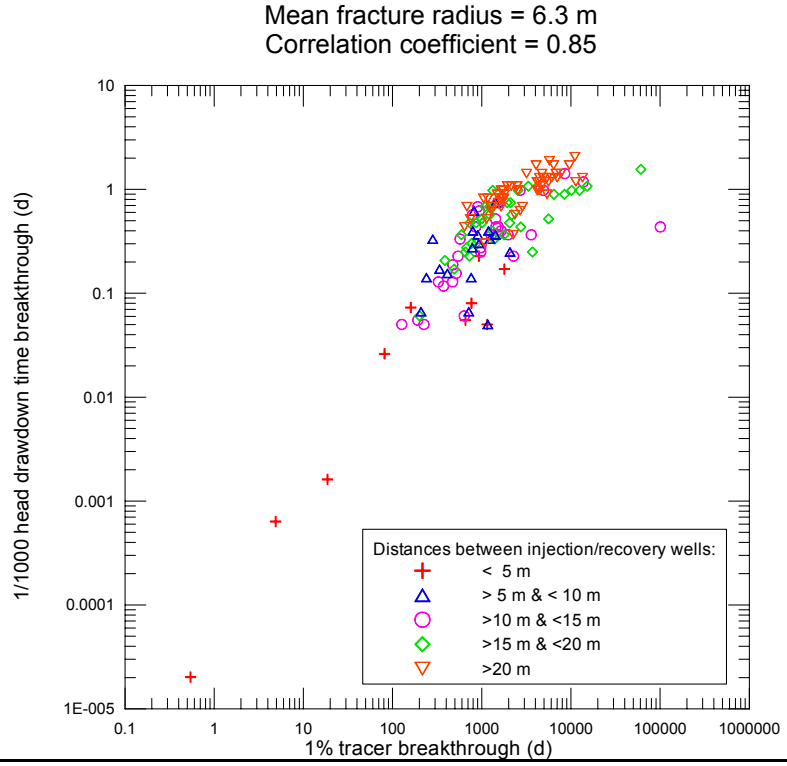

***Figure 2-4:*** *Correlation plot – Mean radius 14.1 m*

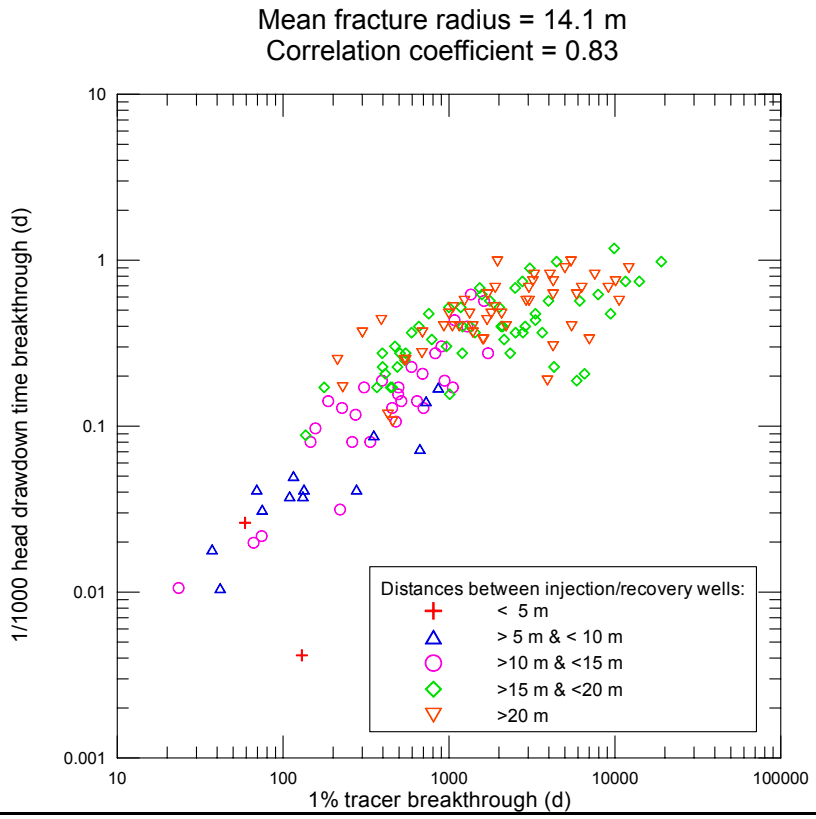


***Figure 2-5:*** *Correlation plot – Mean radius 36.1 m*

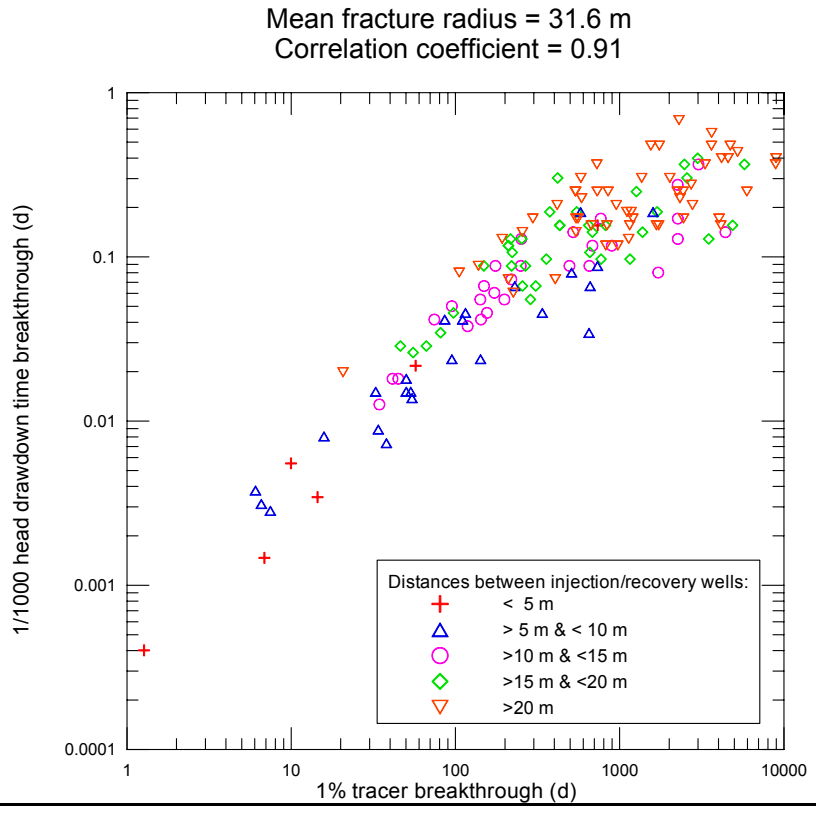

***Figure 2-6:*** *Correlation plot – Mean radius 100 m*

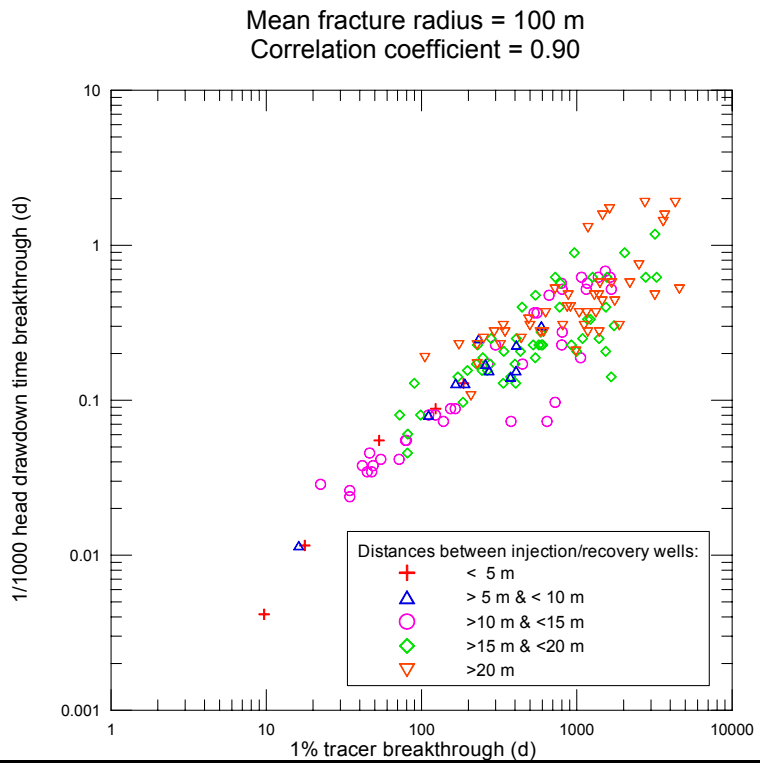


***Figure 2-7:*** *Correlation plot – Mean radius 200 m*

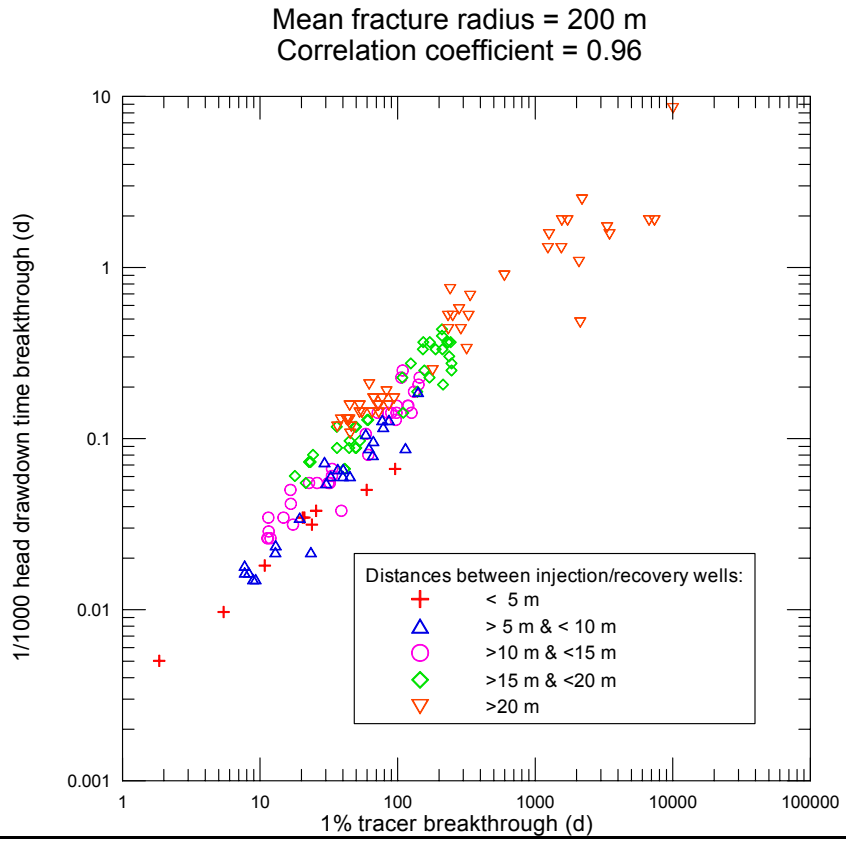

# 3. SIMULATIONS

## 3.1 Description of the runs

Simulations are performed using networks describing the TRUE Block Scale site with 2 different fracture densities: 1.e-5 and 4.e-5 fractures/$m^3$, which lead to fracture mean radie of 141.0 m and 70.7 m respectively. For each network, 2 realizations are made by changing the generating number (seed 1 and seed 2), this in order to assess the impact of the probabilistic process on the results.

Monitoring wells are defined at several radial distances from the production well: 10, 15, 20 or 25 m.

An hydraulic pipe conductivity is assigned to each fracture through a random process constrained by a lognormal distribution of mean: 1.39e-9 $m^3/s$ and standard deviation: 3.88e-8 $m^3/s$. Fracture apertures are defined either constant (1 mm fracture aperture), or correlated to the pipe conductivity through a cubic law relationship (cf. 2.2).

For each realization, a log-log plot of the 1/1000 head drawdown and the 1% particle mass arrivals is built for each monitoring / injection well to investigate if a correlation exists. A sensitivity analysis on hydraulic conductivity is performed in a second step (the ratio between mean and standard deviation is kept constant).

The impacts on the correlation of specific storage and of tracer diffusion into the matrix are also considered.

## 3.2 Constant aperture

In this chapter, the fractured medium is simplified by fixing a constant fracture aperture. The aim is, in a first step, to simulate flow and transport in conditions closer to those of an homogeneous medium and verify if the expected correlations still take place. In a second step, we try to get a better insight on the conditions necessary for getting this correlation and the associated limitations.

### 3.2.1 Mean fracture radii of 141 m

The network realizations generated for the flow and transport simulations are described in Figure 3-1 (seed 1) and Figure 3-2 (seed 2).

The log-log plots of the 1/1000 head drawdown and the 1% particles arrival times show that these two parameters present a linear correlation with a slope of 1 for the different injection points (Figure 3-3 and Figure 3-4). A deviation tends to appear for the latest arrival times (corresponding to particles taking more complex pathways than the propagation of pressure) even for a given radial injection distance with the well.

This correlation is especially clear for seed 2 for tracer breakthroughs earlier than 1e4 days (Figure 3-4). The difference in quality between the two correlations must be linked to the fracture density in the vicinity of the pumping wells, which is denser for seed 1 (Figure 3-3) than for seed 2 (Figure 3-4).

***Figure 3-1:*** *Pipe network for a mean fracture radii of 141 m – seed 1*
View from top of a slice ranging from z = 18 m to 32 m.

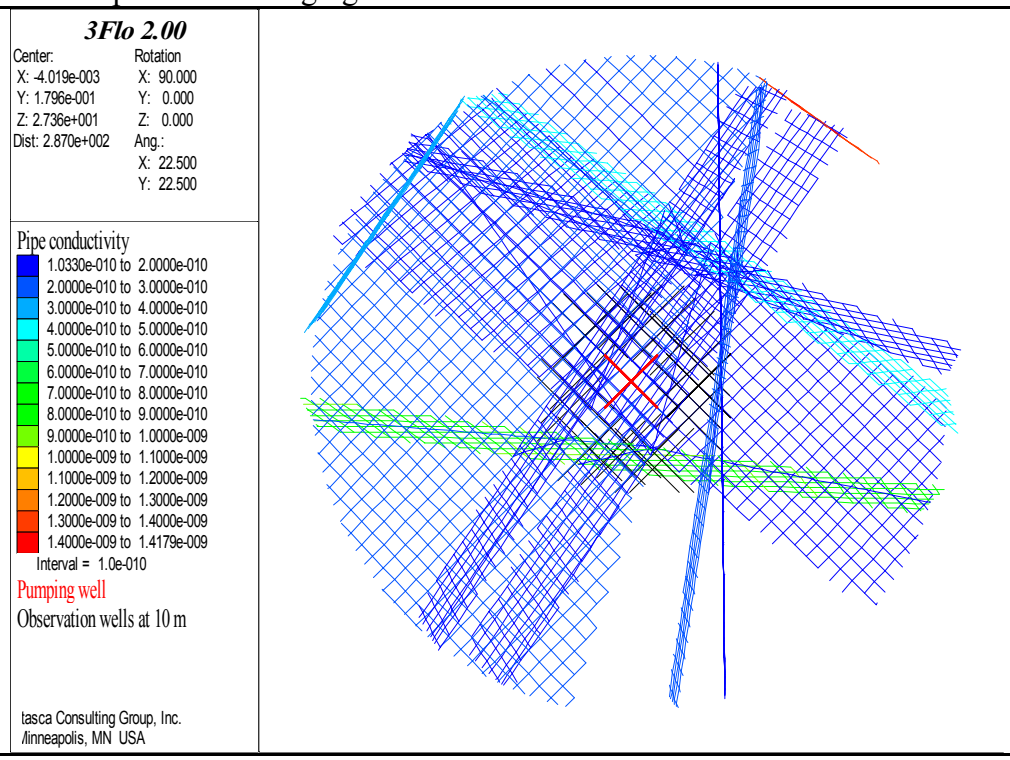


***Figure 3-2:*** *Pipe network for a mean fracture radii of 141 m – seed 2*
View from top of a slice ranging from z = 10 m to 40 m.

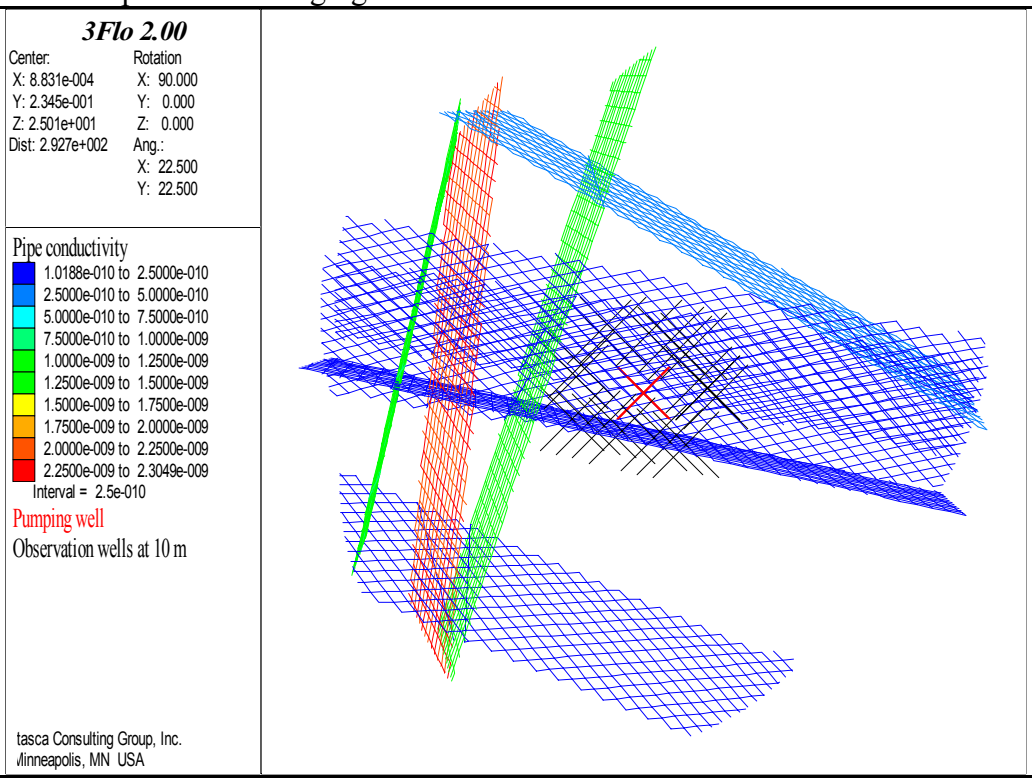

***Figure 3-3:*** *Correlation plot – constant aperture – seed 1 (r = 141 m)*

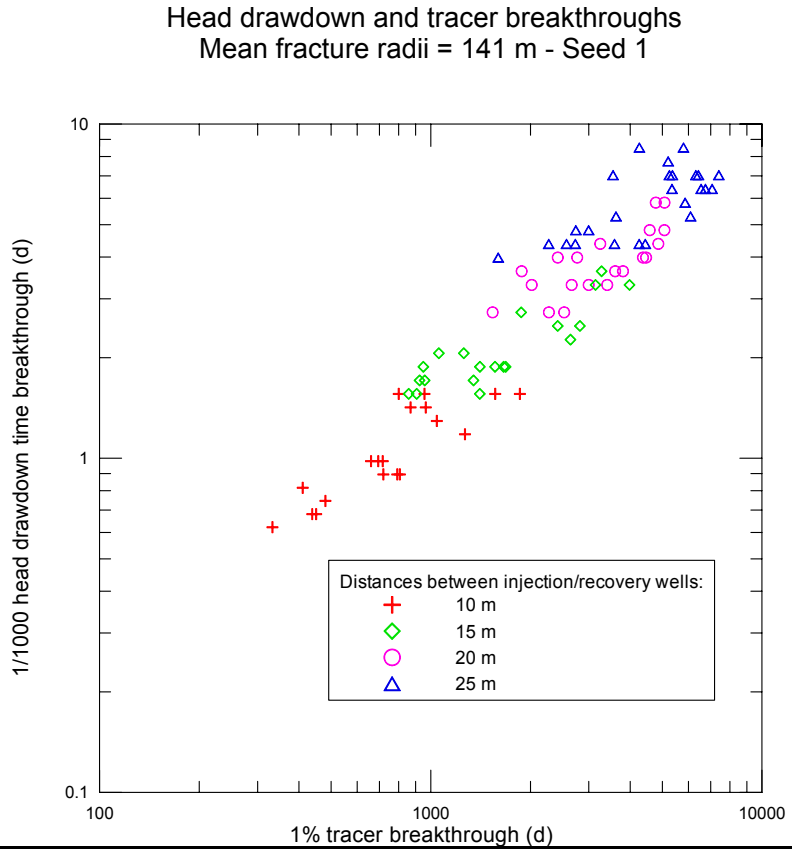


***Figure 3-4:*** *Correlation plot – constant aperture – seed 2 (r = 141 m)*

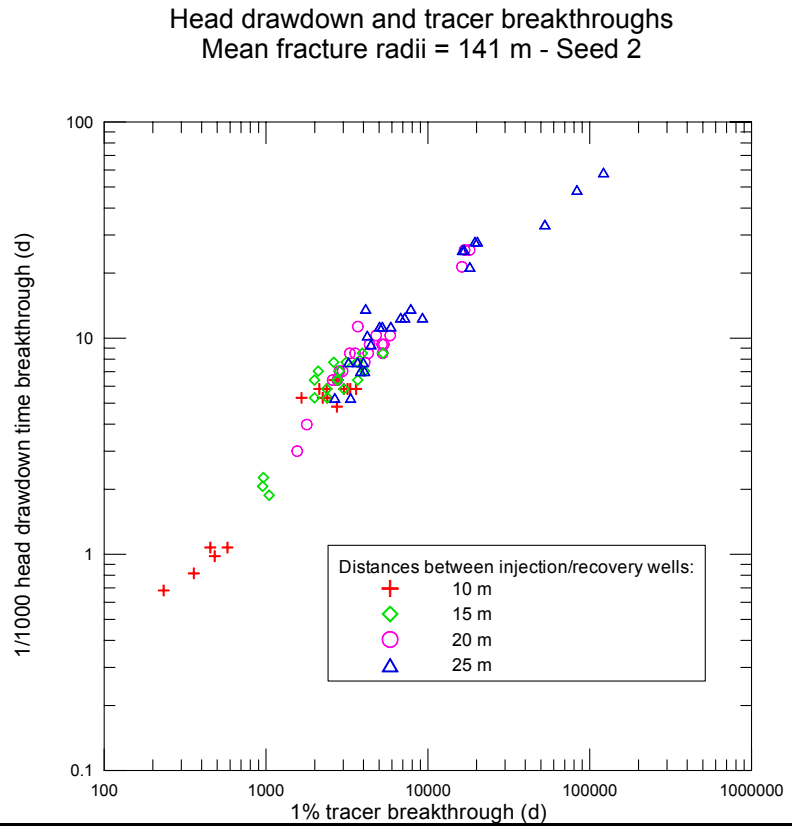

These results are very similar to those published by Herweijer (1996).

Assigning higher values to the hydraulic conductivity (but keeping the variation coefficient constant, that is the ratio "mean over standard deviation", and also keeping the porosity constant) modifies the tracer velocities and the head response with the same ratio. Therefore, this simply shifts the "arrival time – head time" pairs along a unit slope (Figure 3-5 and Figure 3-6). This result is only valid because we are modeling a constant head test. We will also see later that varying fracture apertures (and hence porosities) together with their hydraulic conductivities alters the correlation.

### 3.2.2 Mean fracture radii of 70.7 m

The network realizations used for the flow and transport simulations are described in Figure 3-7 and Figure 3-8.

The relevant log-log plots are displayed in Figure 3-9 and Figure 3-10.

Results are close to those with mean fracture radii of 141 m. One can notice than the correlation is good for seed 1 until arrival times of $10^3$ days (Figure 3-9). For later arrival times, particles are slowed down in relation with the pressure propagation through the formation, only for larger radial distances, i.e. 20 and 25 m. Data for the seed 2 simulation (Figure 3-10) are sparser and the deviation from the unit slope appears earlier and for every radial distance. A careful examination of the two networks shows that injection wells for seed 2 are located in a zone characterized by a much higher density of fractures than for seed 1. Therefore, one can see that the quality and degree of the correlation should depend on the fracture sizes and the rock volume investigated.

Increasing the hydraulic conductivities in the networks (Figure 3-11 and Figure 3-12) shifts the results along a unit slope straight-line, for the same reasons as mentioned above (chapter 3.2.1).

***Figure 3-5:*** *Correlation plot – constant aperture and variable conductivity – seed 1 (r = 141 m)*

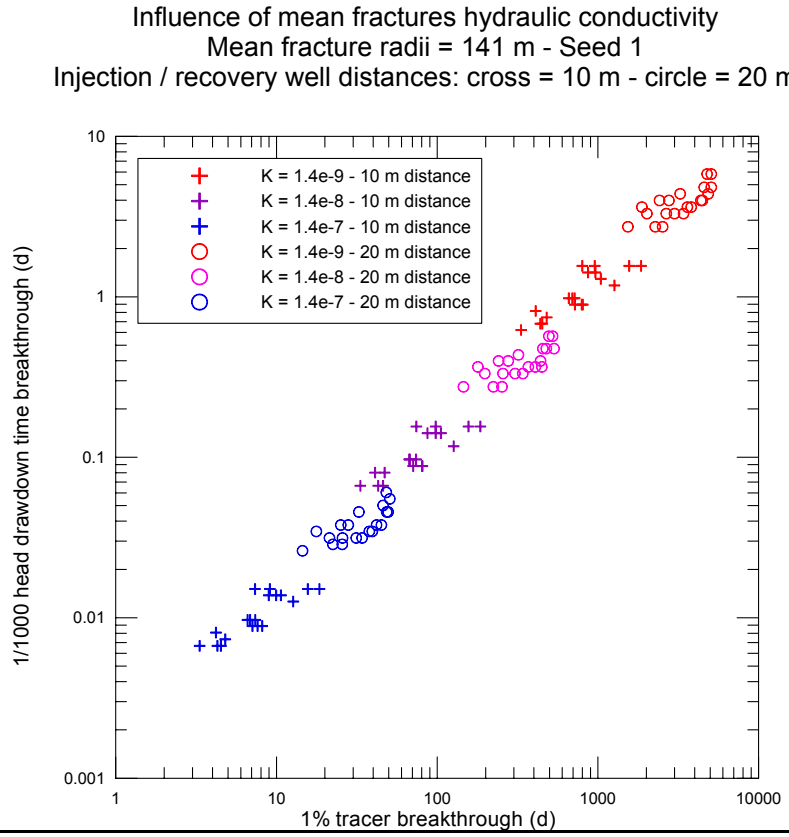


***Figure 3-6:*** *Correlation plot – constant aperture and variable conductivity – seed 2 (r = 141 m)*

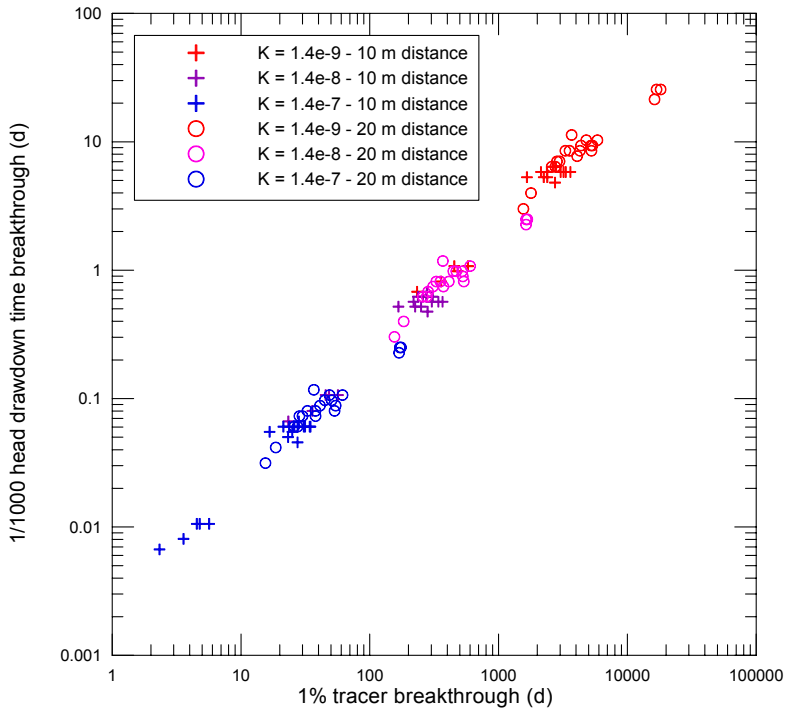

***Figure 3-7:*** *Pipe network for a mean fracture radii of 70.7 m – seed 1*

View from top of a slice ranging from z = 20 m to 30 m.

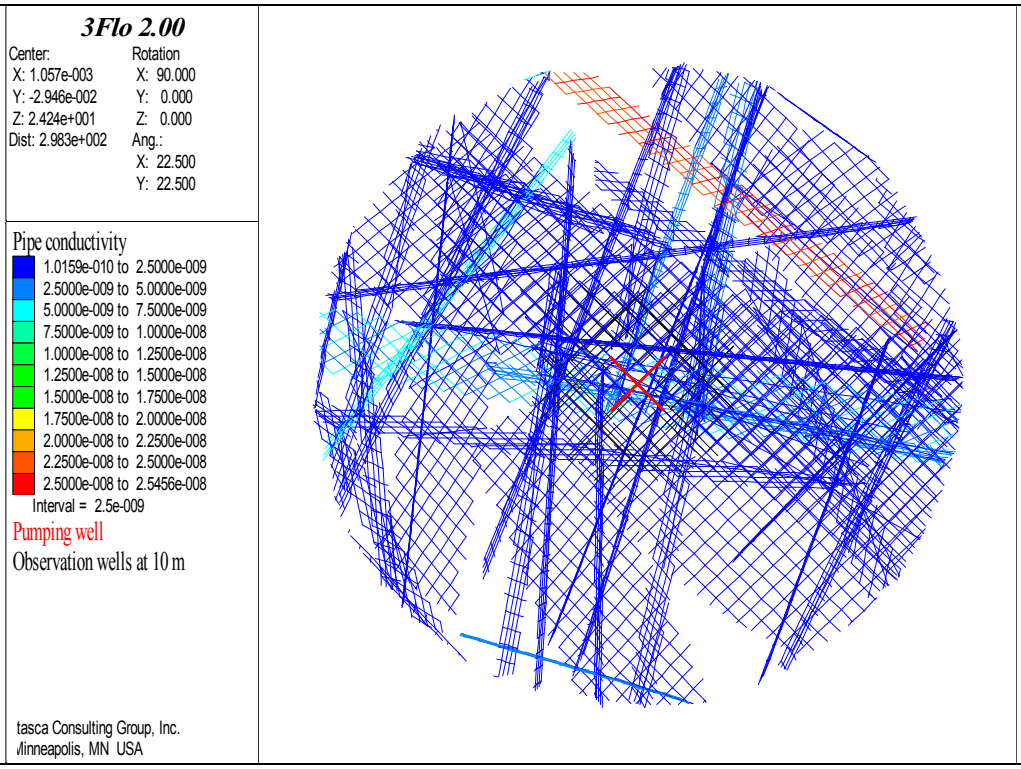


***Figure 3-8:*** *Pipe network for a mean fracture radii of 70.7 m – seed 2*

View from top of a slice ranging from z = 20 m to 30 m.

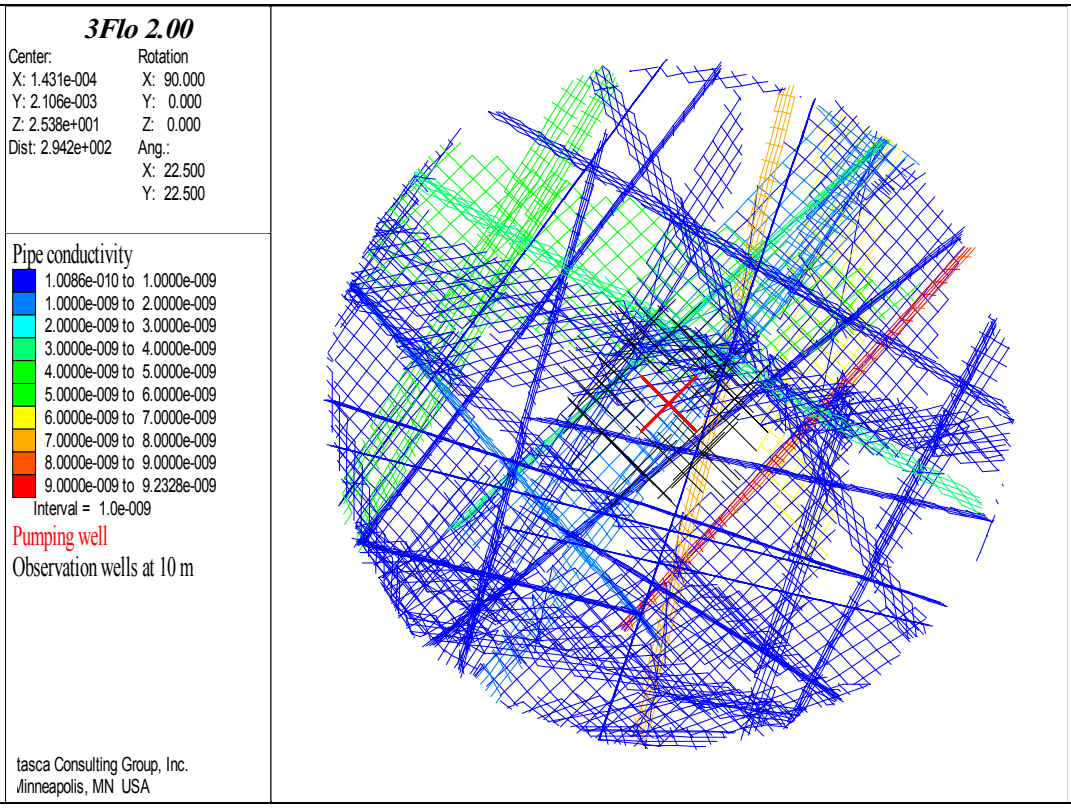

***Figure 3-9:*** *Correlation plot – constant aperture – seed 1 (r = 70.7 m)*

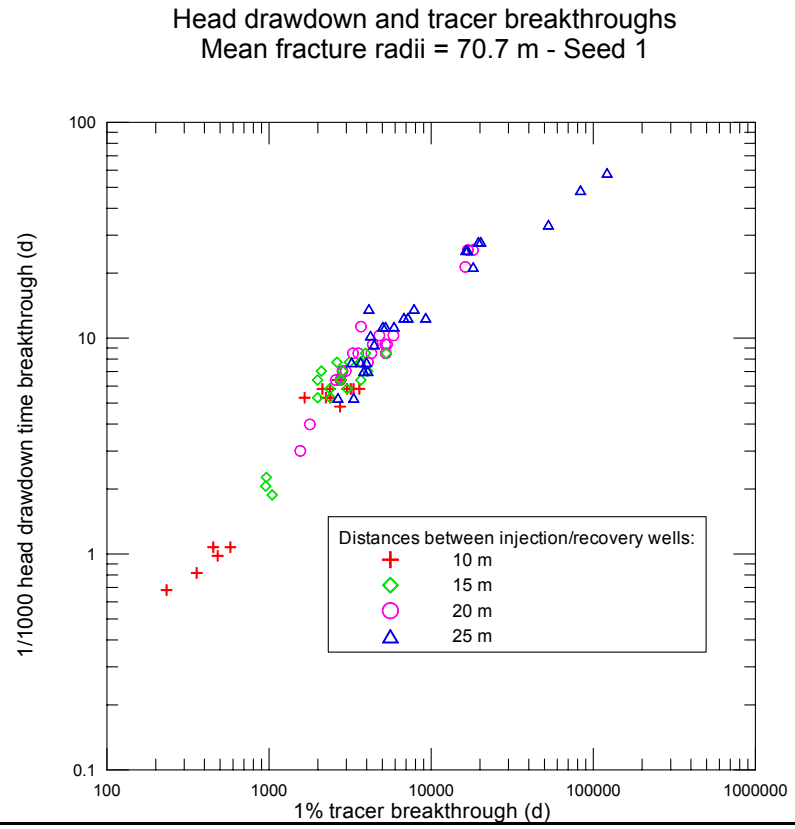


***Figure 3-10:*** *Correlation plot – constant aperture – seed 2 (r = 70.7 m)*

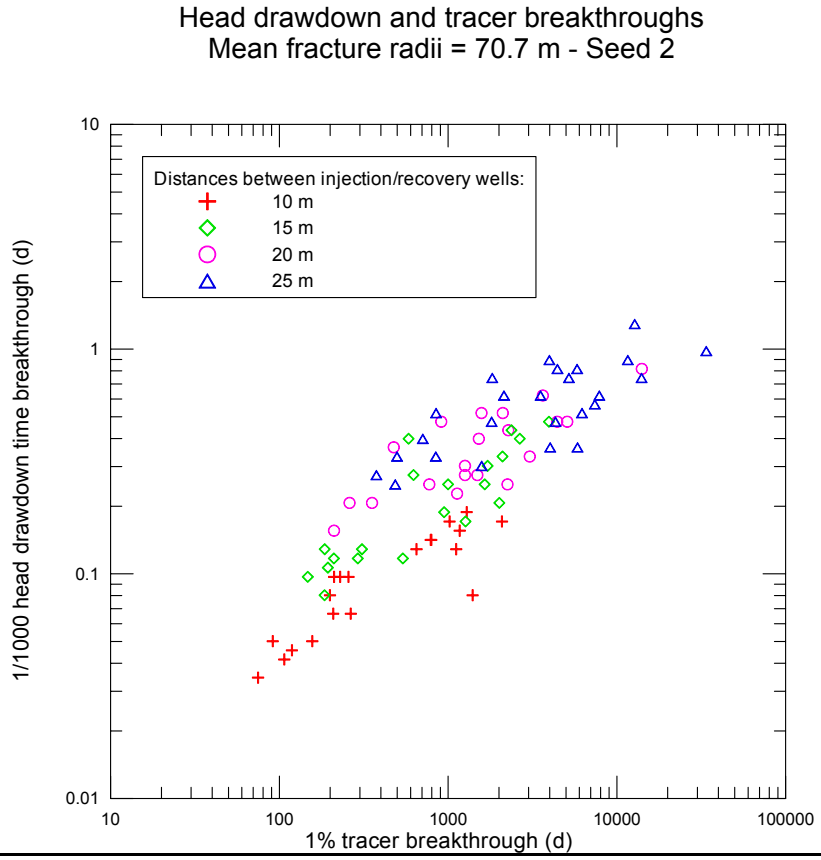

***Figure 3-11:*** *Correlation plot – constant aperture and variable conductivity – seed 1 (r= 70.7 m)*

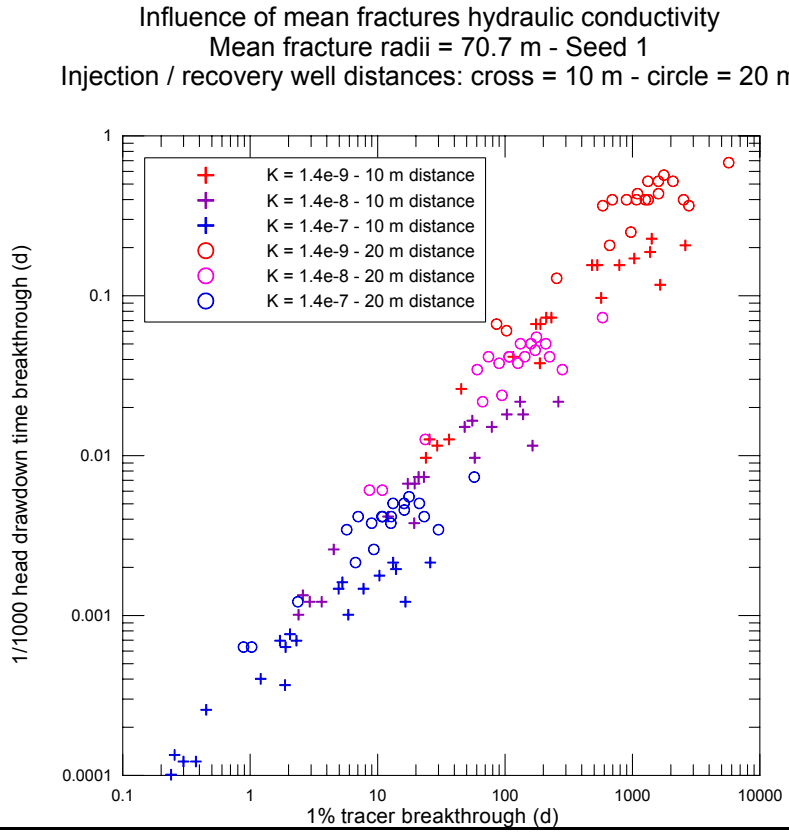


***Figure 3-12:*** *Correlation plot – constant aperture and variable conductivity – seed 2 (r= 70.7 m)*

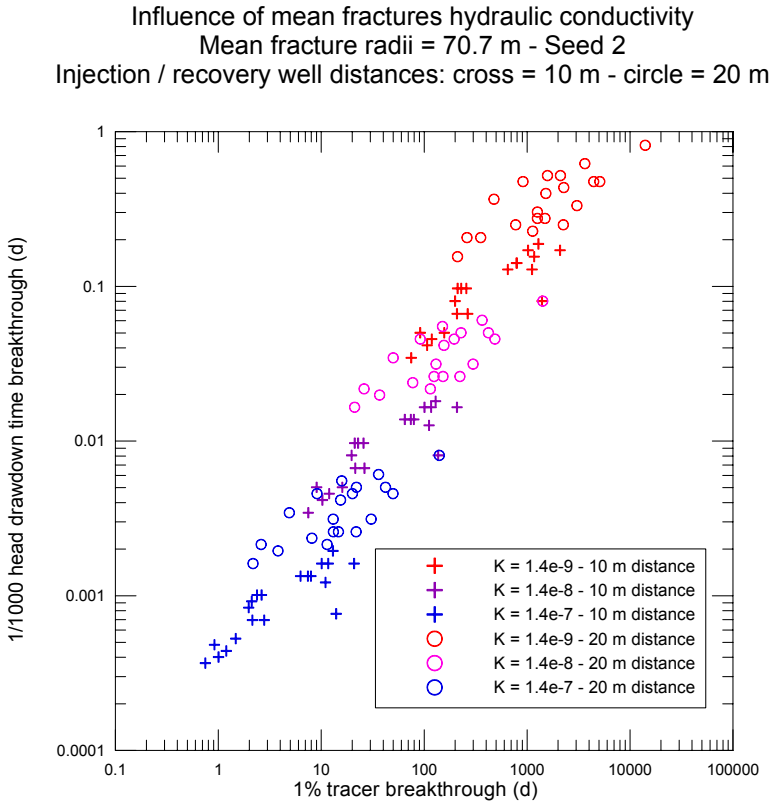

## 3.3 Fracture aperture varying according to the cubic law

The assumption of constant fracture aperture used in section 3.2 leads to a simplified representation of fractured medium flow and transport conditions.

In this chapter, the same networks as before are used but where a "cubic law" relationship between pipe conductivity (C) and aperture (A) is assigned:

$$A = C^{1/3}$$

With this analysis, one can check if the correlations observed can be obtained also in a more realistic medium.

### 3.3.1 Mean fractures radii of 141 m

The simulation results are displayed in Figure 3-13 and Figure 3-14. The correlations are very similar to those obtained with constant aperture which shows that the system geometry between the injection / recovery wells remains the most important factor.

Figure 3-15 and Figure 3-16 show that, unlike simulations performed with constant fracture apertures, we obtain a varying origin for the straight-line correlation depending on mean conductivity of the pipes (Table 3-1). This result is logical because an increase of the conductivity increases the pipe porosity in return and therefore decreases the particle traveling time.

**Table 3-1: Resulting porosity for each hydraulic conductivity value**

| Conductivity ($m^3/s$) | Porosity |
|---|---|
| 1.39e-09 | 1.21e-04 |
| 1.39e-08 | 2.33e-04 |
| 1.39e-07 | 6.24e-04 |

### 3.3.2 Mean fracture radii of 70.7 m

The simulation results are shown in Figure 3-17 for seed 1 and on Figure 3-18 for seed 2 and the influence of varying conductivity is plotted on Figure 3-19 and Figure 3-20.

The curves are similar to those with a mean fracture radii of 144 m, i.e. a good correlation for seed 1 while, for seed 2, a strong deviation from the unit slope can appear even for injection points located at a 10 m radial distance from the pumping well. The effect of the "cubic law" assumption is qualitatively identical to the case of a fracture radii of 144 m.

***Figure 3-13:*** *Correlation plot – "cubic law"– seed 1 (r = 141 m)*

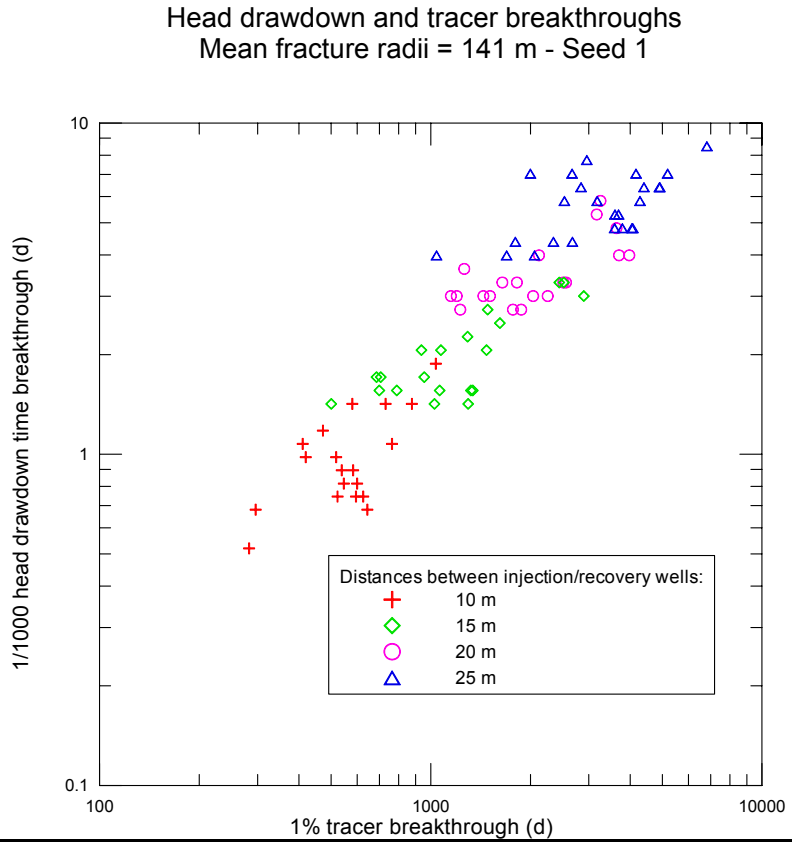


***Figure 3-14:*** *Correlation plot – "cubic law"– seed 2 (r = 141 m)*

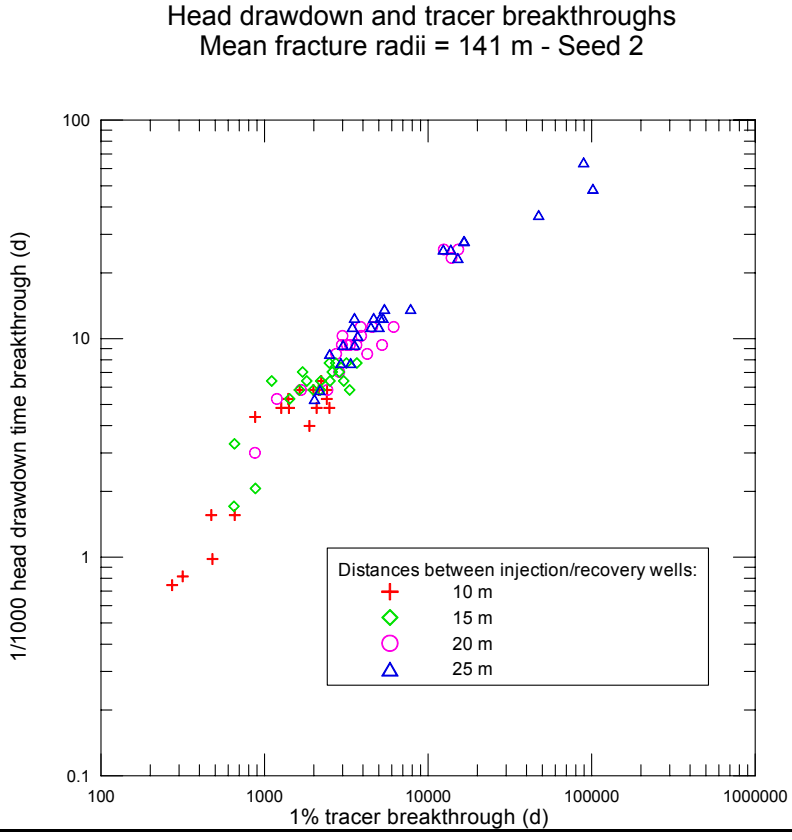

***Figure 3-15:*** *Correlation plot – cubic law" and variable conductivity – seed 1 (r = 141 m)*

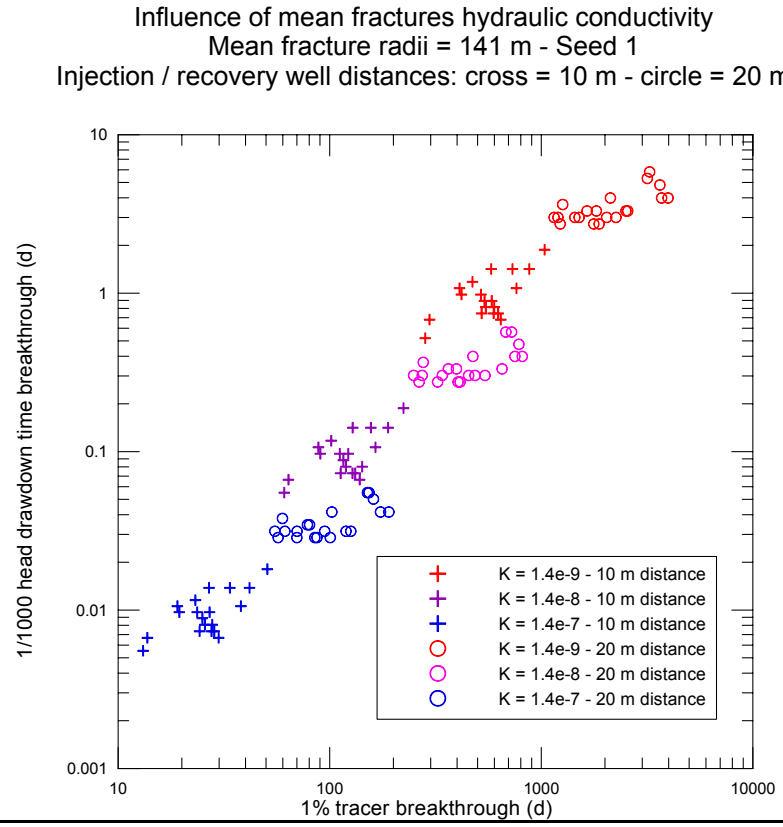


***Figure 3-16:*** *Correlation plot – "cubic law" and variable conductivity – seed 2 (r = 141 m)*

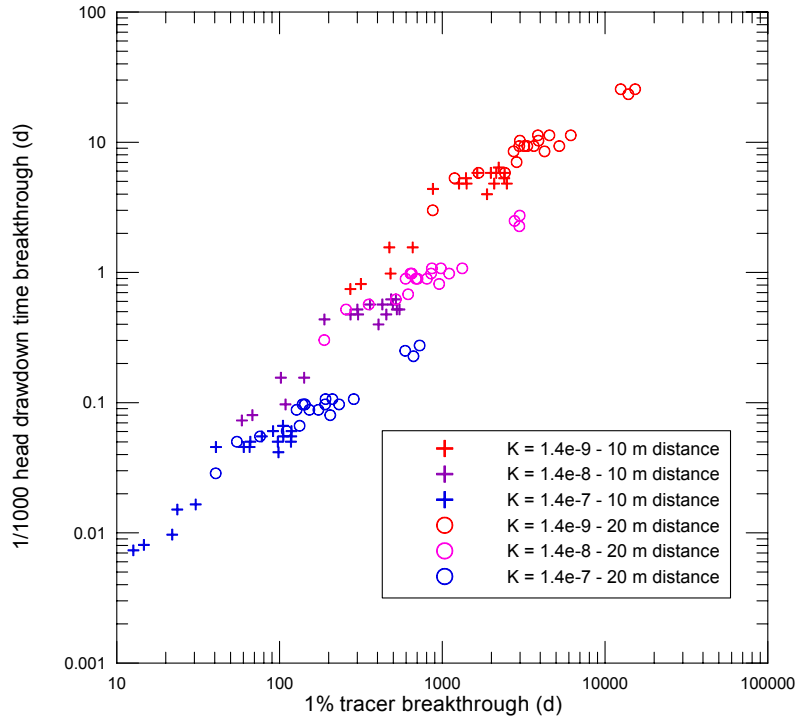

***Figure 3-17:*** *Correlation plot – "cubic law" – seed 1 (r = 70.7 m)*

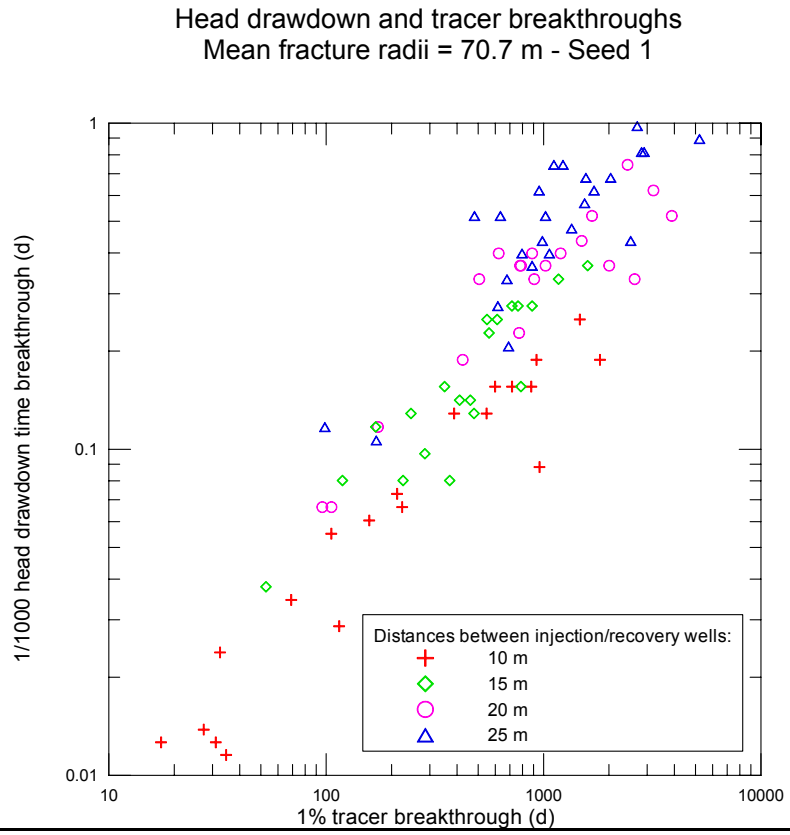


***Figure 3-18:*** *Correlation plot – "cubic law" – seed 2 (r = 70.7 m)*

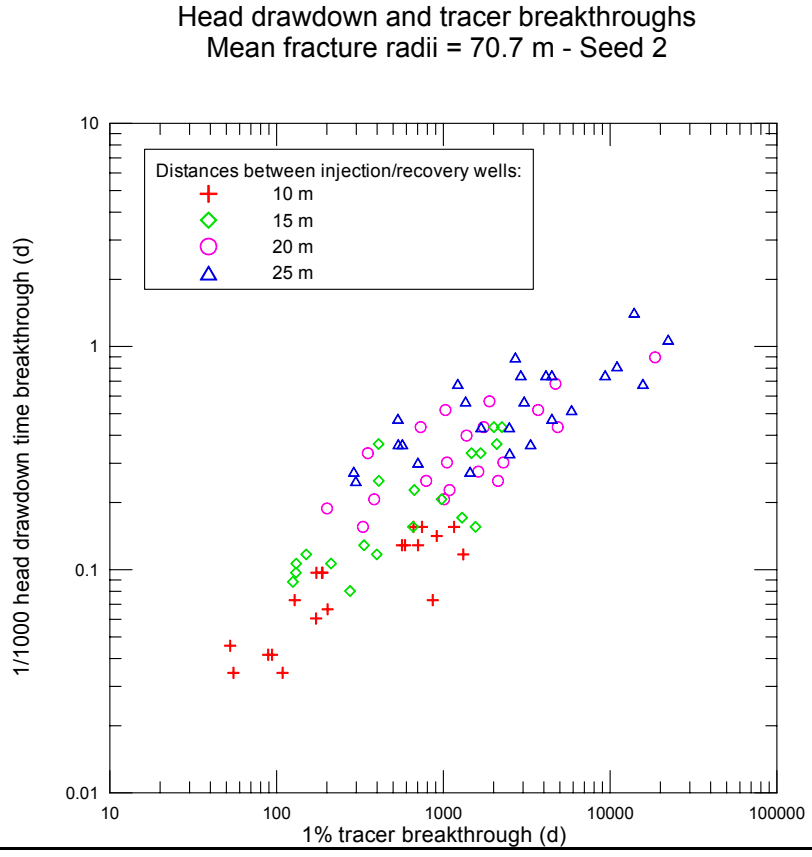

***Figure 3-19:*** *Correlation plot – "cubic law" and variable conductivity – seed 1 (r = 70.7 m)*

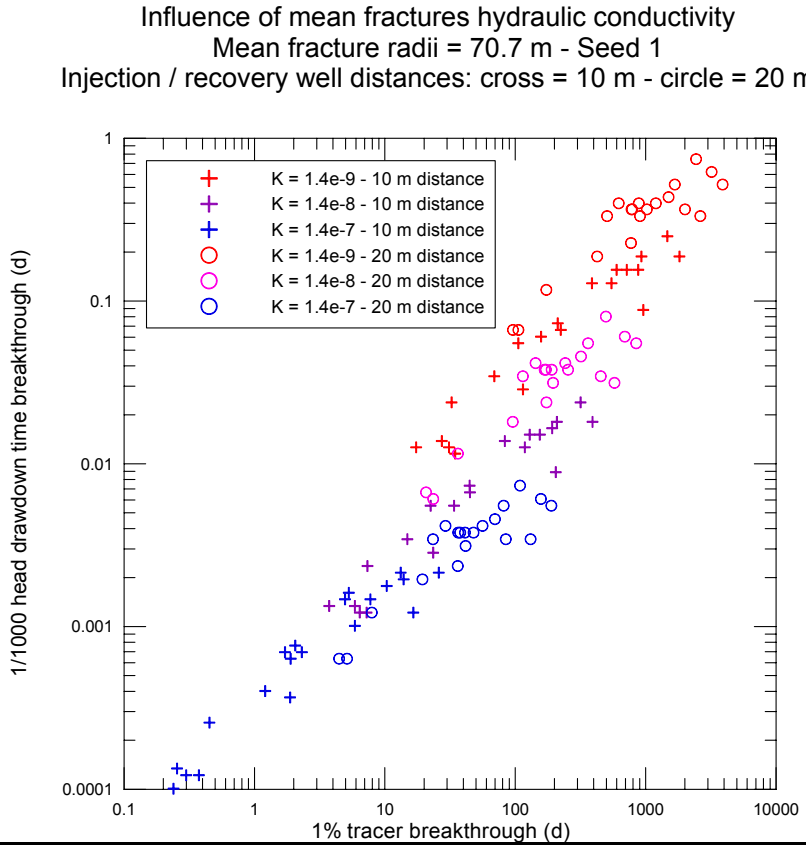


***Figure 3-20:*** *Correlation plot – "cubic law" and variable conductivity – seed 2 (r = 70.7 m)*

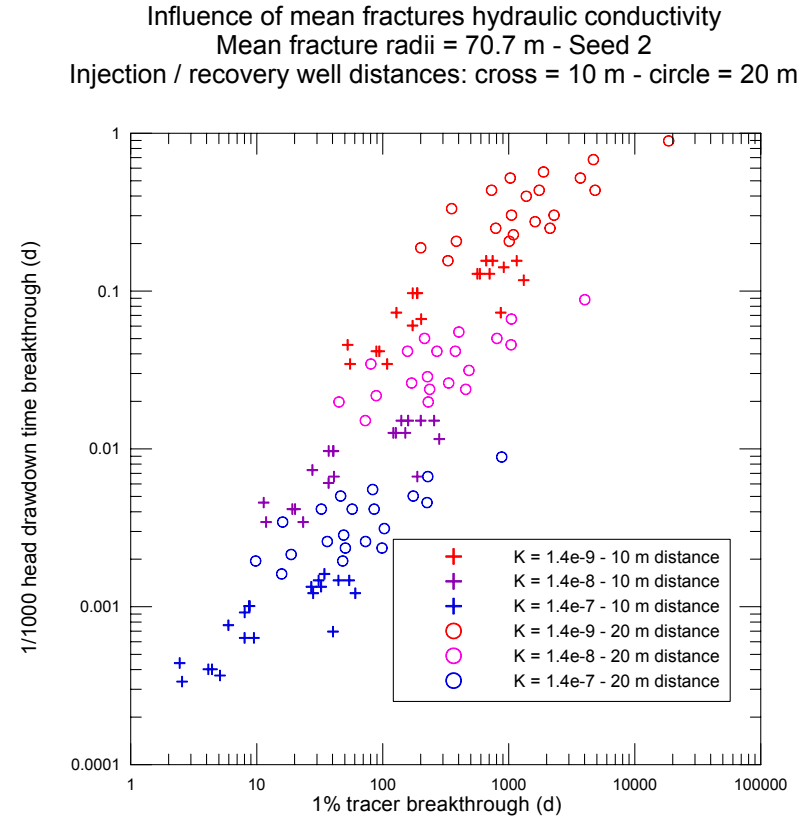

## 3.4 Variable specific storage

In order to complete the check of the main parameters controlling the correlation between pressure drawdown and particle breakthrough times, simulations showing the influence of specific storage (Figure 3-21 and Figure 3-22) are performed. Parameters and conditions of simulations are those described in section 3.3.

Specific storage only affects head drawdown breakthrough and not transport. Results confirm the expected effects that are shifting the unit slope along the head drawdown axis proportionally to the specific storage value.

***Figure 3-21:*** *Correlation plot - cubic law" and variable specific storage (r = 141 m, seed 1)*

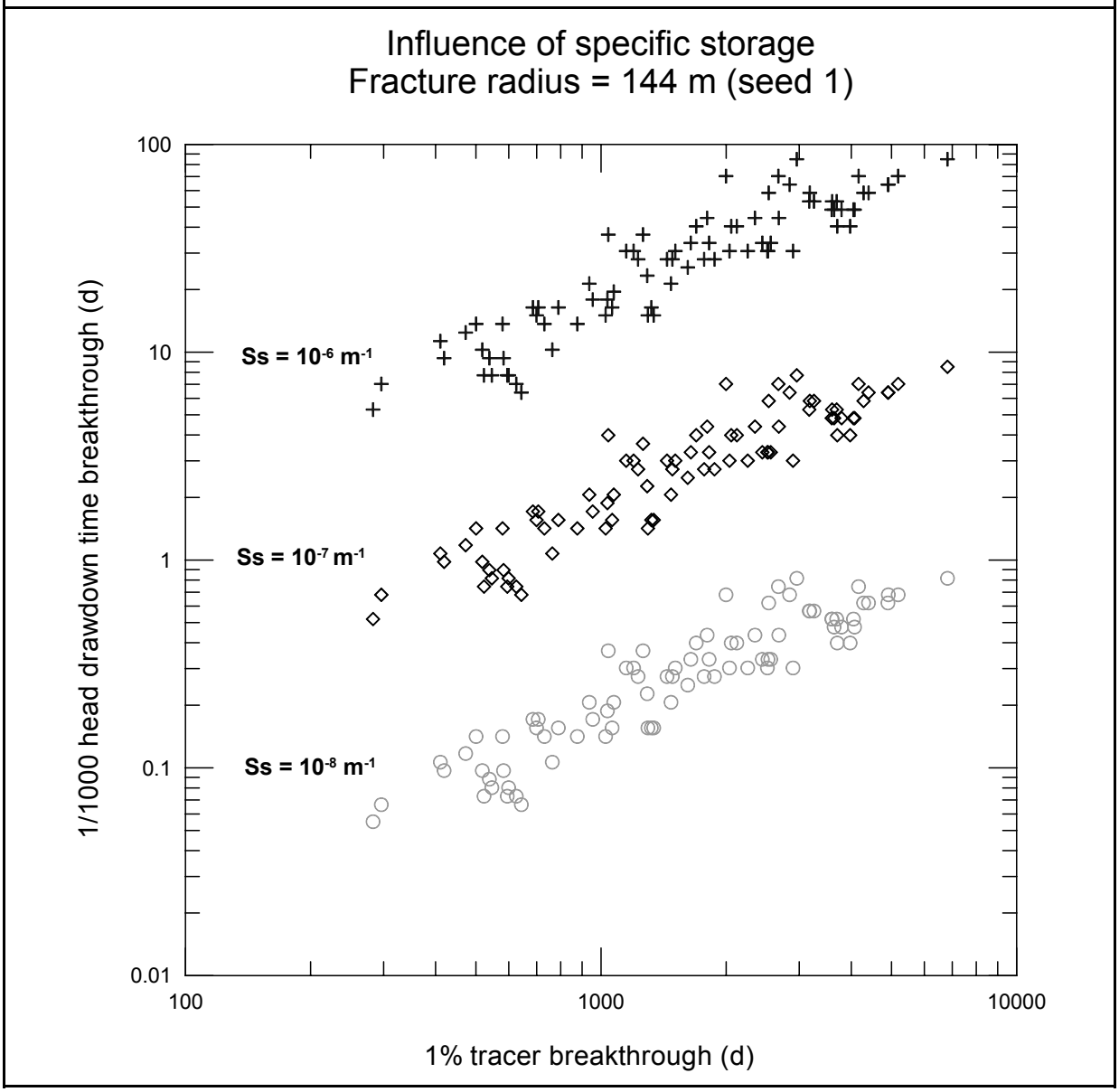

***Figure 3-22:*** *Correlation plot - "cubic law" and variable specific storage (r = 141 m, seed 2)*

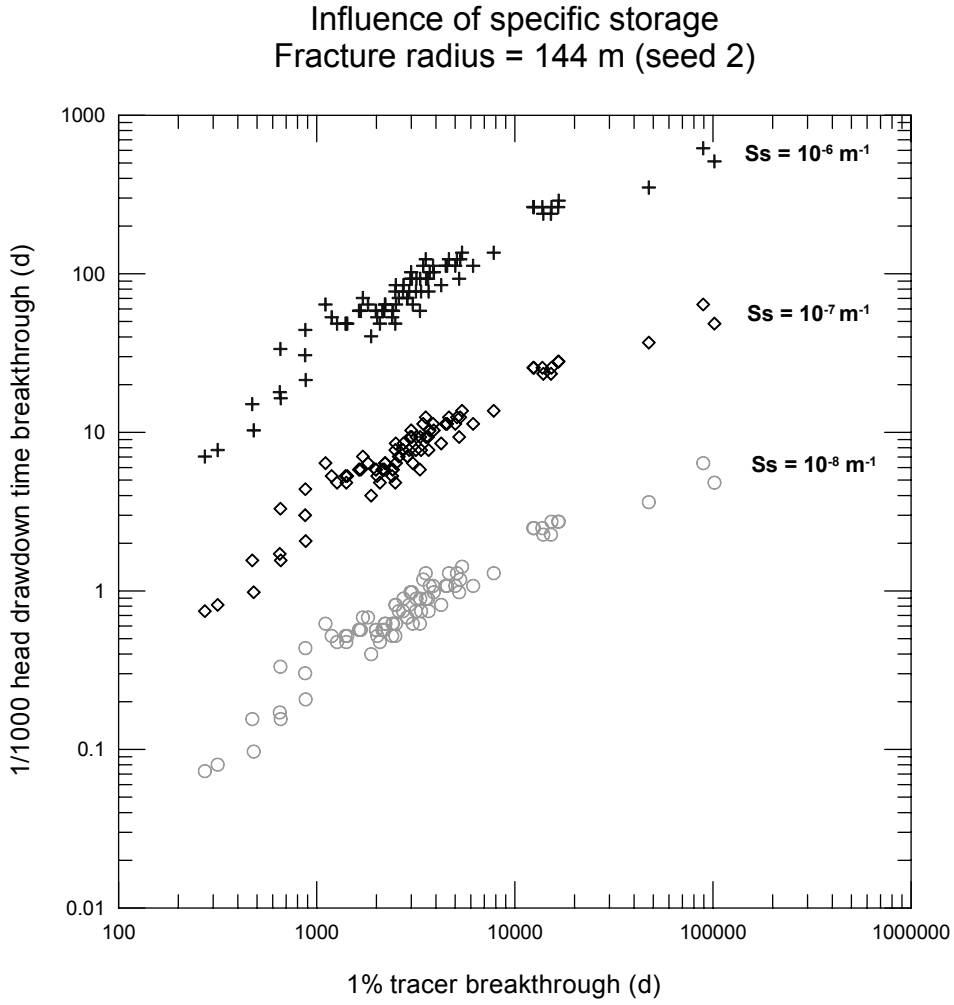

## 3.5 Effects of matrix diffusion

### 3.5.1 Adding matrix diffusion into the model

Retardation through chemical interactions or diffusion into the matrix is likely to disturb the expected theoretical response. In order to assess this impact, we implemented into *3FLO* a simplified version of Fick's law using the *FISH* macro-language. This implementation consists of adding to each pipe an extra number representing the diffused mass into the matrix. At every time step, a function calculates the flux between each pipe and the corresponding diffused mass using Fick's law.

This implementation does not claim to reproduce exactly matrix diffusion processes but provides a tool allowing us to assess the qualitative impact on the correlation of a non-linear retardation effect such as diffusion.

In one dimension, Fick's law states that the mass flux of particles in a fluid is proportional to the concentration gradient:

$$\Phi = - d_0 \frac{\partial C}{\partial x} \qquad \text{Eq. 3.1}$$

Where $d_0$ is known as the molecular diffusion coefficient. Assuming that the process only takes place between the homogeneous pore solution and a single matrix "reservoir" yields:

$$\Phi = - D\left(C_{matrix} - C_{pore}\right) \qquad \text{Eq. 3.2}$$

$D$ being an "apparent" diffusion coefficient. The procedure automatically adds particles to simulate release if there is no particle in the pipe.

### 3.5.2 Comparison of the method with an analytical solution

In order to verify that this simplified Fick law and the implementation into *3FLO* lead to acceptable results with respect to our objectives, we compared a one dimensional simulation to an existing analytical solution given by Tang et al. (1981):

$$C(x,t) = C_0 \, erfc\left( \frac{\varepsilon \, x \, \sqrt{d_0}}{2 a \, u \, \sqrt{t - \frac{x}{u}}} \right) \qquad \text{Eq. 3.3}$$

With:

- $u$: Solute velocity [$m.s^{-1}$]
- $a$ : Fracture aperture [m]
- $\varepsilon$: Rock porosity [-]
- $d_0$ Molecular diffusion coefficient [$m^2.s^{-1}$]

The complementary error function (erfc) is computed with a specialized routine given in Numerical Recipes in C (Pruess *et al.*, 1992).

### 3.5.3 Simulation

The numerical parameters are the following:

| | |
|---|---|
| $u$: | $10^{-3}$ [m.s$^{-1}$] |
| $\varepsilon / a$: | 1 m$^{-1}$ |
| $d_0$: | $10^{-6}$ m$^2$/s |
| $x$: | 75 m |

The Figure 3-23 shows a qualitatively good agreement with the analytical solution. The diffusion coefficient is chosen in order to observe a significant impact of the process. We calibrated a global diffusion coefficient for *3FLO* of $3.10^{-6}$ m$^2$/s close to the one of the analytical solution despite the rough discretization of our matrix diffusion simulator.

***Figure 3-23:*** *Matrix diffusion process - comparaison between an analytical solution and 3FLO*

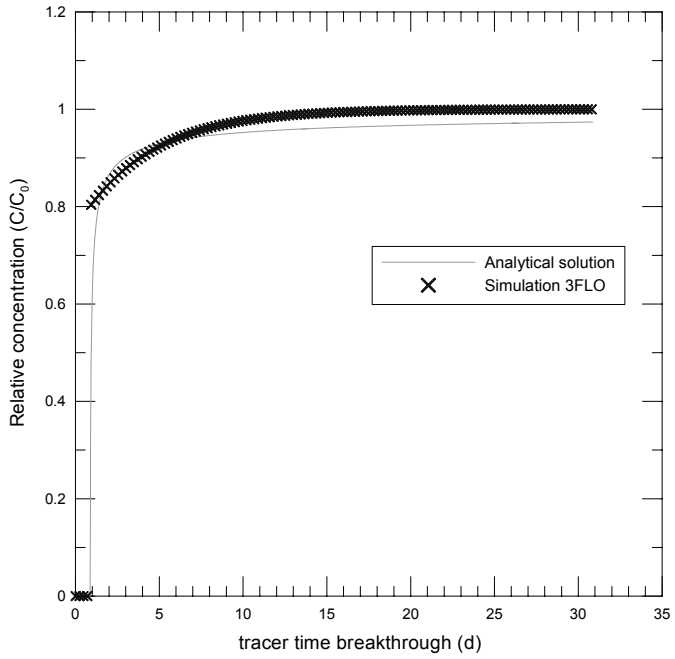


### 3.5.4 Impact of the matrix diffusion

Figure 3-24 shows how matrix diffusion can affect the correlation. It can be seen that the impact essentially exists only for later times.

***Figure 3-24:*** *Influence of the matrix diffusion process*

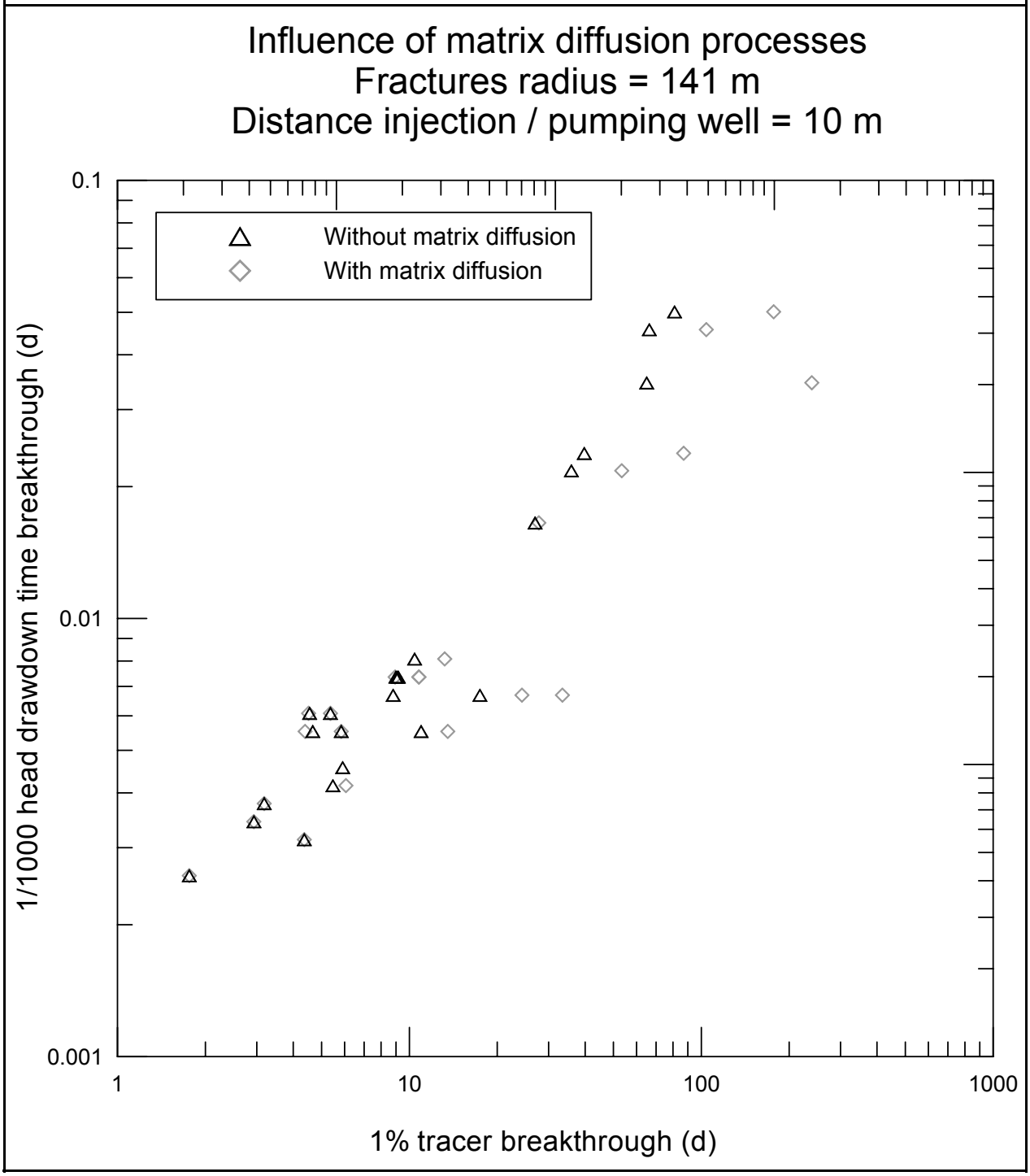

# 4. CONCLUSION

A constant-head hydraulic test (50 m drawdown at pumping well) and conservative tracer tests are simulated in various fracture networks changing both network geometry and conductor hydraulic properties. The breakthrough time for a 0.5 cm drawdown (1/1000) and the arrival time for 1 % of the tracer mass are then compared.

In a fractured medium, it appears that the correlation between small drawdown and first arrival time depends on the respective scale of the fractures and of the volume of rock tested. The network geometry has thus a major influence on the quality of the correlation. In a system with many interconnected small fractures, the pathways between the injection and recovery wells may branch in a lot of different ways, adding some extra tracer dispersion to the transport process, compared to a system with fewer large fractures. This means that for a fracture field with a given "linear density" measured in boreholes, looking at the quality of the correlation obtained between well test responses and tracer breakthroughs should yield information on the significant scale of the fracture network. This in itself would be quite useful, since fracture scales are quite difficult to measure in the field, with size distributions from fracture trace surveys often truncated because of the inadequate size and shape of the available sampling areas (tunnel walls, outcrops).

If varying global system hydraulic conductivities do not affect the correlation, it is likely that a variable conductivity inside each fracture would indeed influence the results. Matrix diffusion or any non-linear retardation phenomenon might also affect the correlation but to a much lesser extent, essentially because we track the early pressure responses and tracer breakthroughs. This conclusion would be very different if, for example, a 50% tracer recovery was monitored.

In terms of a direct field application of the concepts discussed in this report (i.e. "predicting" tracer breakthrough time scales from well tests), one can expect good results if the distance between the monitoring and the pumping wells is not too large. Beside increasing the test durations, increasing distances between wells may add fracture intersections and complexity into the flow and transport system and result into poorer correlations. It is hoped that future adequate well test analysis techniques, using for instance the variable flow dimension approach, will allow us to better understand the system geometry. The information gained from well test analysis would be the key for predicting the correlation between tracer and head draw down breakthrough times and therefore help for designing tracer tests in complex systems.

# BIBLIOGRAPHY

**BILLAUX D., 1990.** Hydrogéologie des milieux fracturés. Géométrie, connectivité, et comportement hydraulique. *Thèse de Doctorat de l'Ecole des Mines de Paris, document du BRGM n° 186*.

**BILLAUX D., and GUÉRIN F., 1993.** "Connectivity and the Continuum Approximation in Fracture Flow Modelling," in High-Level Radioactive Waste Management (Proceedings of the Fourth Annual International Conference on High Level Radioactive Waste Management , Las Vegas, April, vol. 2, pp. 1118-1122. New York: ASCE.

**HERMANSON J., FOLLIN S. & WEI L., 2001** *:* TRUE Block Scale Project – Structural analysis of fractures traces in boreholes KA2563A and KA3510 and in the TBM tunnel. *Swedish Nuclear Fuel and Waste Management Company, Äspö Hard Rock Laboratory, SKB International Progress Report IPR-01-70.*

**HERWEIJER J.C., 1996.** Constraining uncertainty of groundwater flow and transport models using pumping tests, *in Calibration and Reliability in Groundwater Modelling*, *IAHS Publ.*, 237, 473-482.

**PRUESS W.H., TEUKOLSKY S.A., VETTERLING W.T., and FLANNERY B.P., 1992.** Numerical recipes in C. *Cambridge University Press*, 994 p.

**TANG D.H., FRIND E.O., and SUDICKY E.A., 1981.** Contamined transport in fractured porous media: analytical solution for a single fracture. *Water Resources Research 17 n°3, p. 555-564*.

# APPENDIX

***3FLO***
**3D Flow and Transport code in porous and/or fractured media**

## NAME, VERSION and ORIGIN OF THE CODE

3FLO, Version 2.0
Developed by ITASCA Consultants S.A., France

## GENERAL DESCRIPTION

*3FLO* is a software applied to the 3D simulation of flow and transport in porous and/or fractured media. *3FLO* can solve various types of problems :

- Flow in fracture networks, represented by a 3D network of pipes, or one-dimensional channels.
- Flow (saturated or not) in porous media :
  - ✓ Using classical (Galerkine) 3D Finite Elements, or
  - ✓ Using Mixed-Hybrid 3D Finite Elements.
- Flow in interacting fractures and porous media.
- Pollutant transport, simulated by the particle tracking method.
- Geochemistry, coupled or not with solute transport, taking into account most types of reactions.
- Mathematical morphology, for analyzing the geometrical properties of fractured media.

*3FLO* can also be used to perform fracture network statistical studies (i.e. : orientation, size, transmissivity, etc... distributions). It also provides a complete logic to process geometrically fracture and pipe networks, in order to "trim" them. For example, a command can be used to discard all dead-ends (useless if the problem at hand is only steady-state).

## FEATURES of *3FLO*

### *FISH* macro-language

One unique feature of ITASCA codes is the FISH macro-language. This language can be used to create new variables, meshing procedures, particle detection procedures, specifically designed graphical output, to develop any type of statistical distribution for use in fracture generation or other, and so on.

**Fracture generation, and assignation of conductivities**

*3FLO* generates a 3D network of pipes on any assembly of planes:

- Generation of a network of flow planes, with any shape, and detection of their intersections,
- On each plane, generation of a network of regularly spaced or Poisson distributed channels,
- Connection of the channels from one plane to another, through the fracture intersections, to constitute the pipe network.

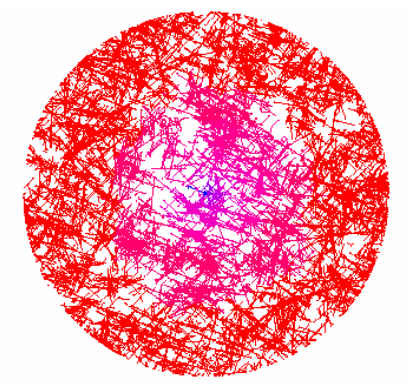

A 3D fracture network

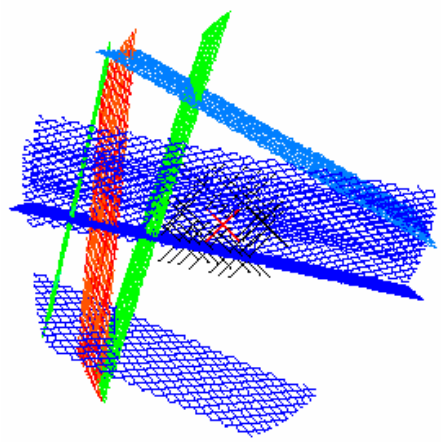

*Color-coded conductivities of fractures*

Once a network is built, one can assign to each pipe a conductivity taken from a statistical distribution (constant, uniform, normal, lognormal -truncated or not-, or any other distribution to be programmed in *FISH)*.

An aperture map known in an image format (pixels) can also be simulated using a grid of pipes.
The Mathematical Morphology module can quantify the geometrical properties of the space between the fractures (size, shape, connectivity distributions, and so on).

**3D mesh generation**

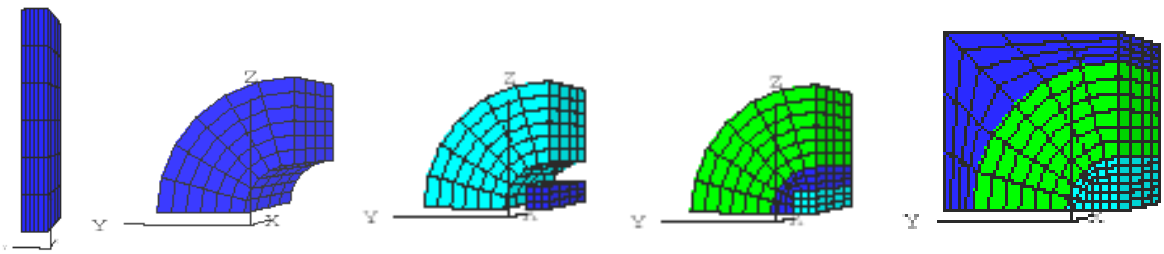

*Successive steps to obtain a desired 3D geometry*

3FLO's power lies in applying to its basic hexahedron or tetrahedron shapes the *FISH* macro-language. Using it, one can reshape, duplicate, join, delete, and so on, the basic building blocks, and thus create a 3D "jigsaw puzzle" that fills the final geometry of the model.

**Flow simulations**

*3FLO* computes steady or transient flow in :

- ✓ 3D fracture networks,
- ✓ 3D porous media (steady or transient flow, saturated or not),
- ✓ 3D fracture networks coupled with porous media.

The flow equation is solved in 1D classical Finite Elements for fractures, and in 3D Mixed-Hybrid Finite Elements for porous media. These elements are more precise than classical (Galerkine) 3D elements, and allow a proper computation of face fluxes. This helps minimizing solute transport computation errors. For example, flow and transport problems are solved without difficulty in models with permeability contrasts of $10^7$.

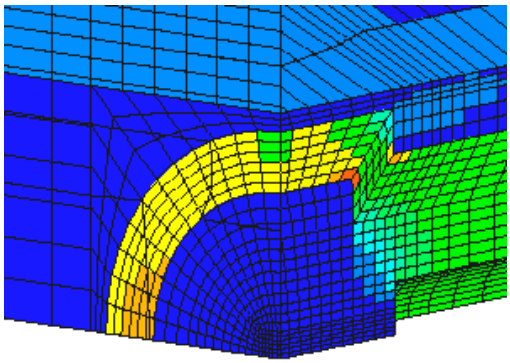

*Average flow velocities in a nuclear waste storage model. Permeability contrast is $10^7$ between plug (blue) and periphery (yel-green)*

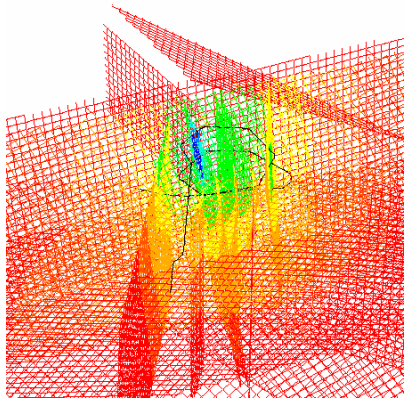

*Heads due to the excavation of the access drift to the Äspö (Sweden) underground laboratory*

**Solute transport**

*3FLO* simulates solute transport using the Random Walk method. In 3D fracture networks, flow is one-dimensional everywhere in pipes, except at intersections. Dispersion is therefore only longitudinal, and is "completed" by the full mixing occurring at intersections. In 3D elements, once the flow field is known, the movement of a particle can be separated in :

- ✓ a longitudinal displacement along a flow line, simulating advection and longitudinal dispersion, and
- ✓ two orthogonal transversal displacements simulating transversal dispersion.

Diffusion can also be represented.
Solute transport may be simulated in "mixed" model, with both fractures and a porous medium. 1D-3D interaction may then receive special treatment.

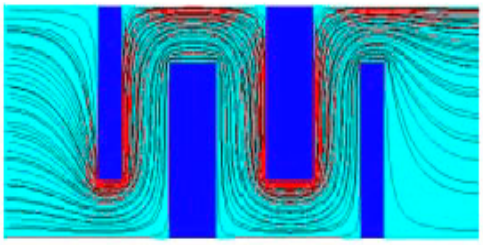

*Particle tracks in a theoretical validation example. The permeability ratio between the two materials is $10^7$*

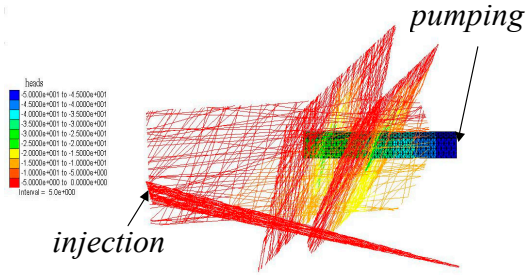


*Heads in a coupled fractures-and-continuum model*

## Geochemistry, and coupling with transport

*3FLO* can account for most types of reactions: precipitation, dissolution, adsorption, oxydo-reduction, kinetics.

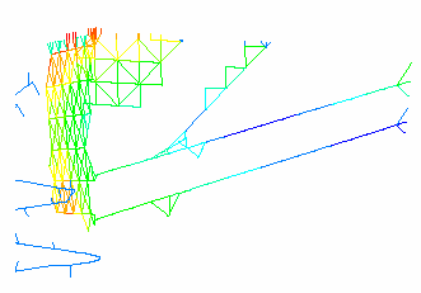

*pH in a fracture network*